KU LEUVEN

FACULTY OF ECONOMICS AND BUSINESS

Financial Risk Modeling

Practical applications towards risk-centric portfolio management

Vermeir Jellen
r0595545

Thesis submitted to obtain the degree of

MASTER OF FINANCIAL AND ACTUARIAL ENGINEERING

Promotor 1: Prof. Dr. Peter Leoni
Promotor 2: Prof. Dr. Wim Schoutens

Academic year: 2015-2016

Contents

Preface

To be added

Leuven, 29/06/2015.

Chapter 1

Introduction

Financial markets have historically been plagued with a multitude of financial crises and black swan events. Recent occurrences of such events entail the Russian debt crisis of '98, the bursting of the dot-com bubble in 2000, the sub-prime mortgage crisis of 2007 and the ongoing European sovereign debt crisis. All these crises had an enormous effect on financial markets: They caused an upsurge in volatility that went hand in hand with declining asset prices and the destruction of financial wealth. From a risk and portfolio management perspective, these worst case events must be taken into account and their potential future realizations must be anticipated. Hence, it is necessary to devise and employ methods and techniques that are able to cope with these empirically observed extreme fluctuations in the financial markets.

1.1 Problem statement

Portfolio managers strive to make optimal investment decisions for their clients while managing the overall risk-return profile of their portfolio. In general, the goal of this asset allocation process entails generating maximum returns while obtaining minimal exposure to downside risk. Indeed, the key (μ, γ) paradigm proposed by Markowitz[1] is still considered as the anchor point for portfolio optimization. However, it remains a big challenge to assess the riskiness of an asset and to effectively measure portfolio diversification and dependencies between multiple assets.

A portfolio manager has many statistical and econometric tools at his disposal for both risk evaluation and portfolio optimization. In general, such portfolio optimization tools take risk and return estimates as input and their goal is to output optimal weight allocation between assets. However, due to their underlying normality assumptions, many of these classical portfolio management tools return incorrect or sub optimal results. The models fail to adequately capture the underlying asset return properties. To alleviate these problems, portfolio managers must cope with the empirically observed asset return characteristics during all phases of the portfolio management process. Hence, the stylistic features and dependency structure of the underlying assets must be taken into account to evaluate portfolio risk in a reliable way.

Additional challenges are encountered during the formulation of the portfolio optimization models and the calculation of their respective input parameters. For example, the classical optimization models such as the Markowitz Portfolio framework utilize sample estimators which assume normality of asset returns and are very sensitive to outliers. In practice, precautions must be taken to both minimize the estimation risk of these estimators and robustify the optimization models themselves. Many more practical considerations come to mind. An institutional portfolio manager may want to put limits on certain downside risk metrics or incorporate risk diversification constraints in the optimization process. Portfolio managers also face the challenge of incorporating their own views and strategies in the portfolio optimization process. Hence, the asset allocation process should be robustified across multiple trading strategies to allow for optimal tactical asset allocation.

1.2 Thesis outline

This thesis aims to give a broad overview on the state of the art regarding both financial risk management and robust portfolio optimization. The methods and techniques under consideration mainly consist of a recombination of already existing statistical concepts and robust convex optimization procedures that are applied to finance-related problems. Pfaff 2013[2] and Fabozzi et al.2007[3] have written complete textbook expositions including a comprehensive literature overview on the subject matter. Naturally, both these sources are heavily referenced inside this work with regard to the theoretical concepts. However, the added value of the current work aims to be of a more practical nature. Indeed, the goal of this thesis is to derive useful tools from the theoretical concepts and illustrate and apply the techniques in a realistic setting in such a way that industry professionals can directly benefit from them.

This thesis is divided into three main parts. After the current introductory chapter, we focus our attention to the risk modelling aspects of the portfolio management process. We offer motivational examples on why one should stay clear of the normality assumption while assessing portfolio risk. Stylized facts of univariate and multivariate financial market data are presented and discussed. We follow up with a few definitions and interpretations on financial risk and focus our attention to the Value at Risk (VaR) and Expected Shortfall (ES) measures. In the remainder of this chapter we present alternatives to the normal distribution for modelling and forecasting the latter risk measures. We give an exposition on the Generalized Hyperbolic Distribution (GHD) and introduce methods and concepts from extreme value theory (EVT) as a means of capturing severe financial losses. Next, conditional risk measurements are presented in the form of GARCH models and copulae are discussed with the purpose of modelling multivariate dependencies between assets. From a more practical point of view we perform out of sample backtests to evaluate the risk forecasting performance of the models. Here, we argue that a mixed EGARCH-Clayton/Gumbel copula model is especially suitable for asset return modeling and risk forecasting at the portfolio level. We conclude the chapter with a demonstration on how the concept of 'VaR targeting' can be employed as a

useful tool for providing superior risk adjusted returns.

In the second part we discuss and apply some recently proposed portfolio optimization techniques. Naturally, we start with a theoretical introduction on the Markowitz Portfolio framework. Next, we introduce robust portfolio optimization techniques as a remedy against the outlier sensitivity encountered by the classical model. Here, we employ a suite of robust estimators for the first and second moments to mitigate estimation risk of the estimators: Theoretical simulations and out of sample mean variance (MV), tangency and global minimum variance (GMV) backtests are performed to assess the performance of the estimators. Next, we discuss robust portfolio optimization methods that directly facilitate the inclusion of parameter uncertainty inside the model specification. Finally, we manage to avoid the use of moment estimators altogether by including the complete market distribution into a portfolio optimization model. More concretely, the market distribution consists of mixed Clayton-Gumbel copula simulations and they are included into a minimum conditional value at risk (CVaR / ES) optimization model.

In the third and final chapter, we focus our attention on tactical asset allocation and practical trading constraints. A few simple trading strategies are discussed and the tools from the previous chapters are employed to mix trading signals together in a robust and risk-optimal fashion. Next, we investigate the importance of transactioncosts and lotsize constraints. To mitigate transactioncosts we propose a two layer optimization model that allows the individual strategies to trade among eachother. Rebalancing of the optimal target weights occurs when a statistically significant change in the underlying portfolio weight structures is detected. As an extension, we argue that this final optimization framework is flexible enough to also include dedicated high frequency or statistical arbitrage strategies that do not allow for weight mixing. To accomplish this, these particular strategies can be considered as individual assets and they must implement their own dedicated transactioncost optimizers. As a final practical consideration, we end the chapter with a discussion on how to convert the Interactive Brokers floating tier transactioncost structure into a mixed integer program.

Chapter 2

Financial market data and risk measurement

In order to adequately asses and model financial risk we must first investigate the properties and characteristics of the underlying market data. These properties are summarized in the literature as 'stylized facts' (see Campbell et al. 1997[4]; McNeil et al. 2005[5]) and they have important implications for risk management models. More concretely, in order to derive reliable risk measures, a risk model must capture the underlying time series characteristics of the financial data adequately well. In this chapter we summarize both the univariate and multivariate asset return properties and illustrate them with empirical data.

2.1 Stylized facts for univariate asset return series

The stylized facts for univariate asset returns can be summarized as follows:

- Time series data of asset returns are not independent and not identically distributed.
- The volatility of the asset return process is not constant with respect to time. Extreme events are observed closely together (volatility clustering).
- The absolute (or squared) returns are highly autocorrelated.
- The distribution of returns is leptokurtic and left skewed. Large negative returns are more likely to occur than large positive returns.

For illustration purposes, we utilize daily timeseries of the S&P500 index (SPY) and the Ageas stock price (AGS) as our sample data. The first timeseries represents a composite index that contains a weighted average of many underlying stocks. The second timeseries represents the stock price of a Belgian insurance company that was heavily hit during the 2007 sub-prime mortgage crisis. Figure 2.1 and Figure 2.2 illustrate the

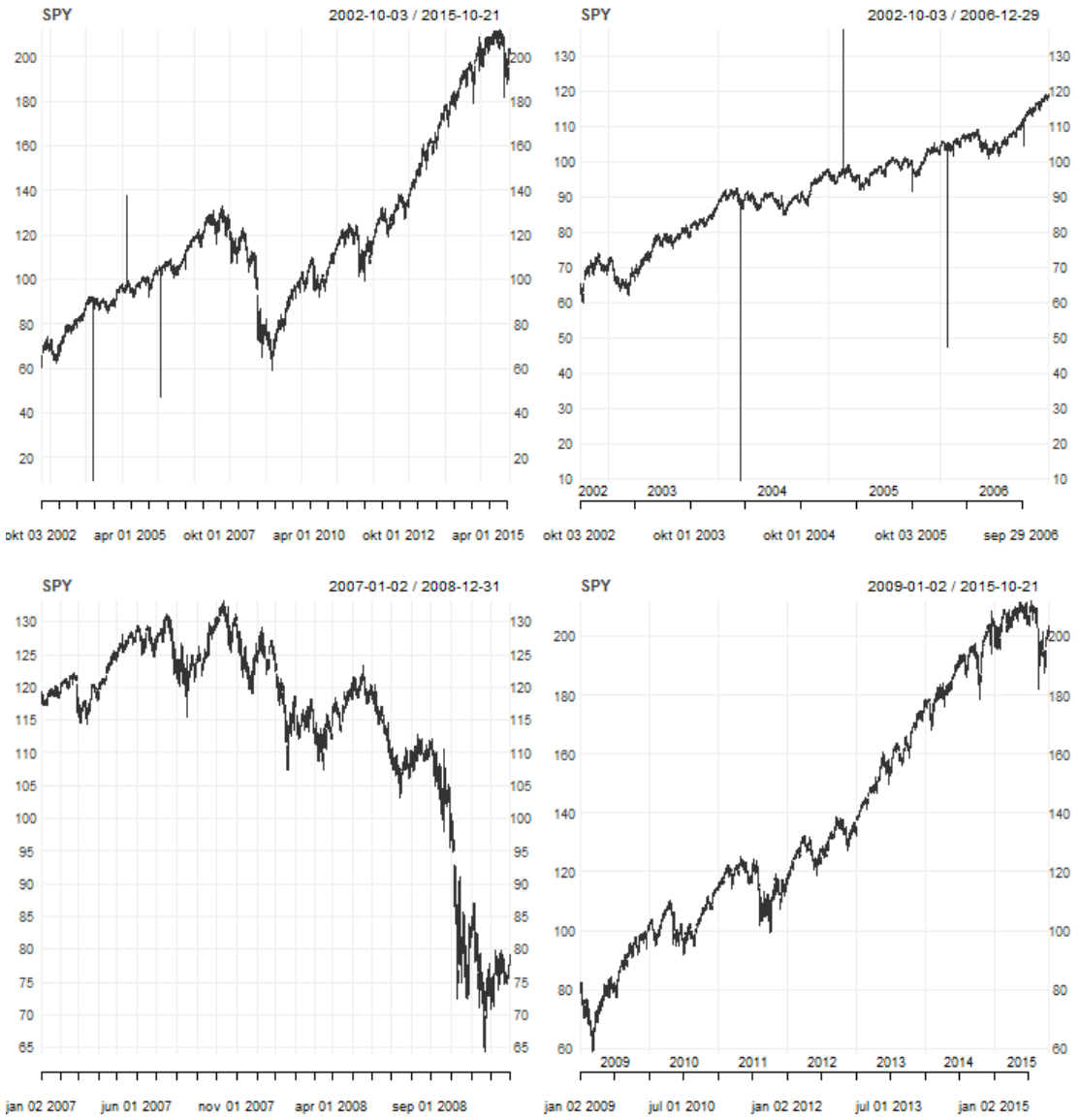

Figure 2.1: SPY - Timeseries

timeseries plots for SPY and AGS respectively. Note that the top left plot displays the complete time-interval under consideration while the other three plots provide subviews on smaller time-intervals.

Figure 2.3 and figure 2.4 illustrate the stylistic features of SPY. The top left graph in figure 2.3 illustrates the volatility clustering behavior of the asset returns and shows a big volatility cluster centered around the sub-prime mortgage criss period. On the top right graph, the boxplot clearly implies heavy tails but a potential left skewed dis-

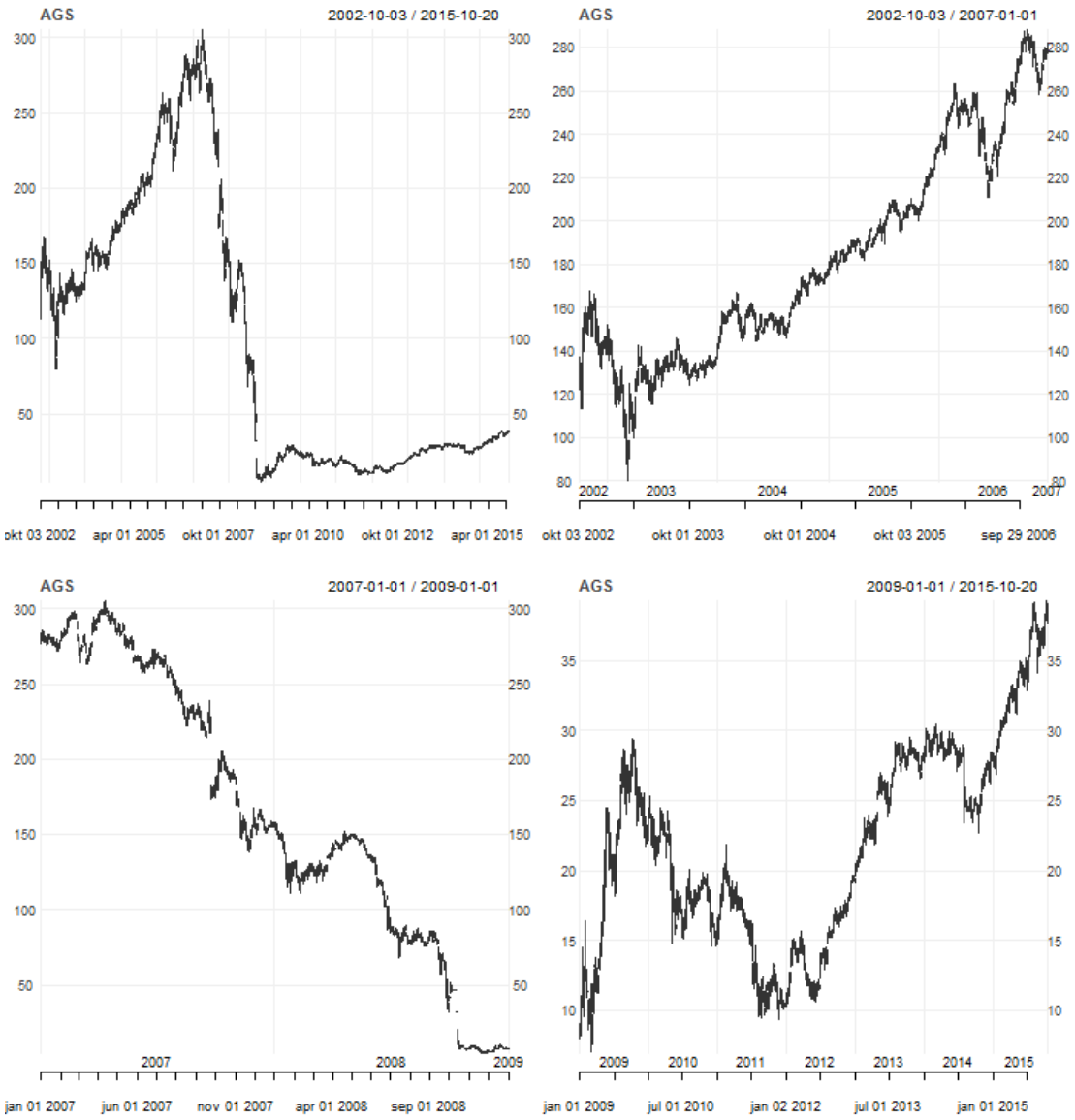

Figure 2.2: AGS - Timeseries

tribution is not readily apparent. However, statistical analysis shows that the data is effectively left skewed: The skewnesss is -0.21 and the excess kurtosis lies around 11.63. The ACF and PACF graphs in the bottom plots hint at a slight first or second order autocorrelation of asset returns. In comparison, the top two plots in figure 2.4 illustrate that the autocorrelations and partial autocorrelations of the absolute returns are significantly different from zero and taper off only slowly. The bottom left graph shows a quantile-quantile plot of the returns compared to the normal distribution and makes the

heavy tails apparant. The bottom right graph shows the 100 largest absolute returns and illustrates that they are clustered together, implying once again the existence of volatility clustering.

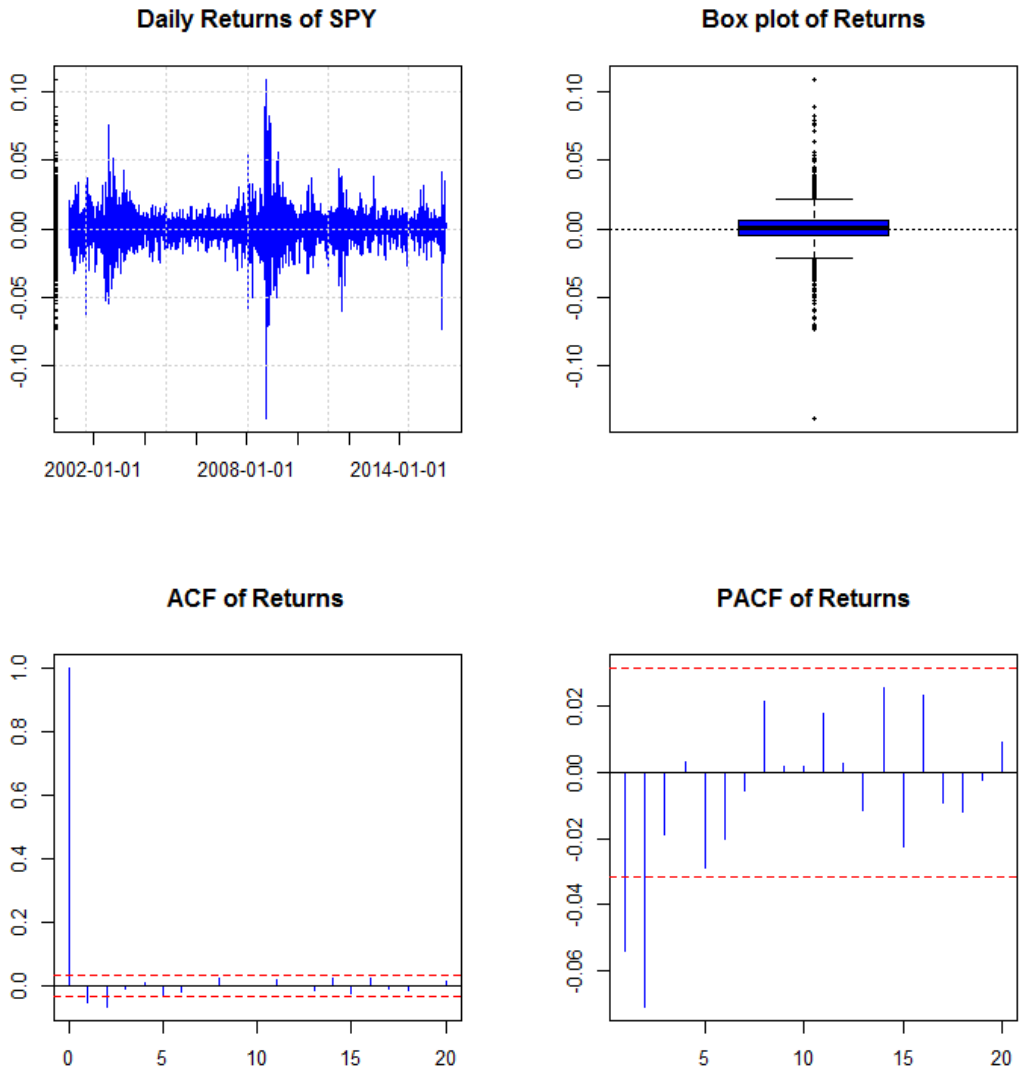

Figure 2.3: SPY - Stylistic features

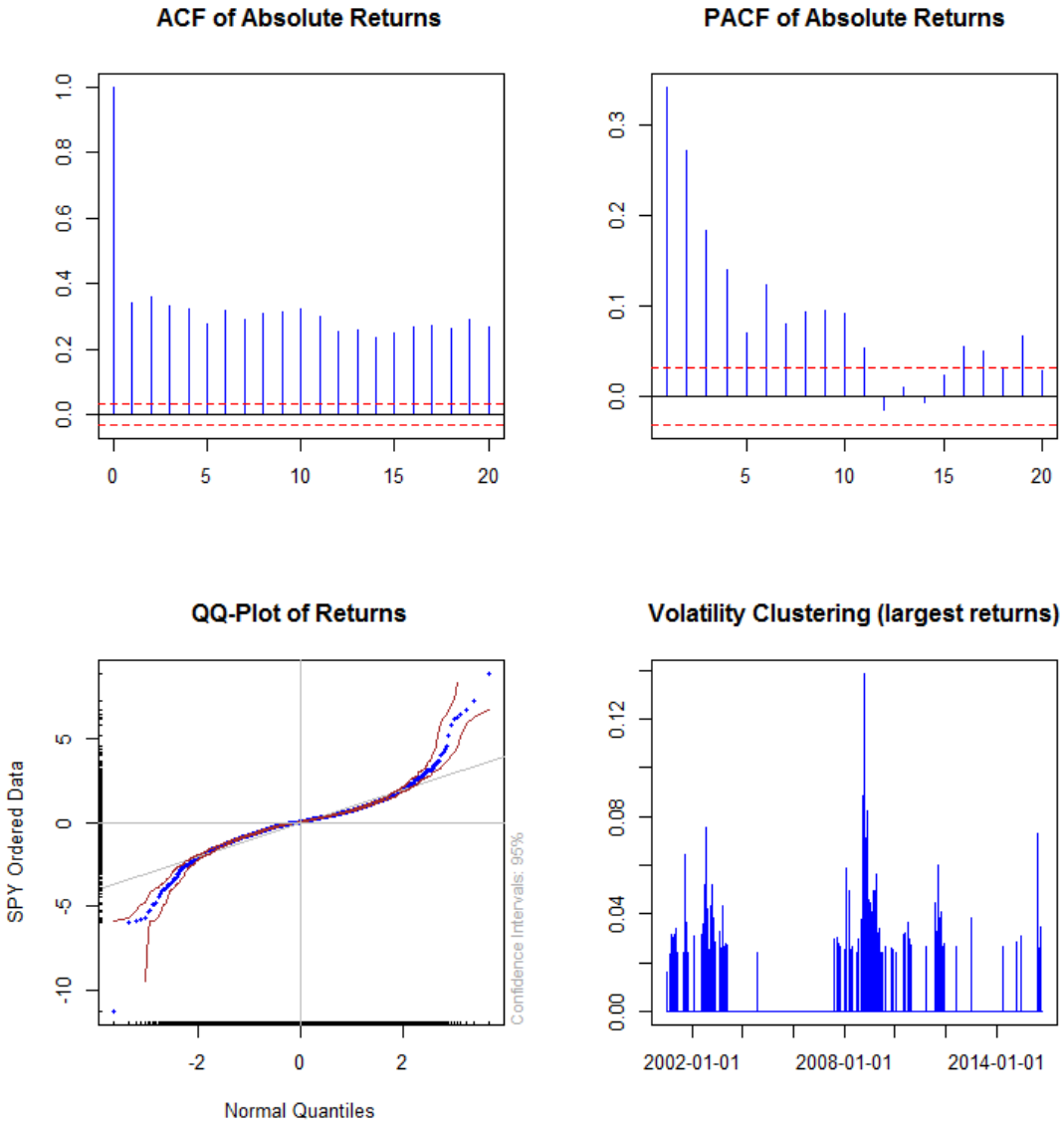

Figure 2.4: SPY - Stylistic features

Figure 2.5 and figure 2.6 illustrate the equivalent graphs for the AGS stock. We notice that the stylistic features of this individual stock are even more pronounced than for the S&P index. The skewed negative tail and corresponding skewness coefficient of -2.99 are immediately apparent in the respective box -and quantile-quantile plots. The return data shows an excess kurtosis of 67.59 and the volatility is clustered even more heavily around the sub-prime mortgage crisis period.

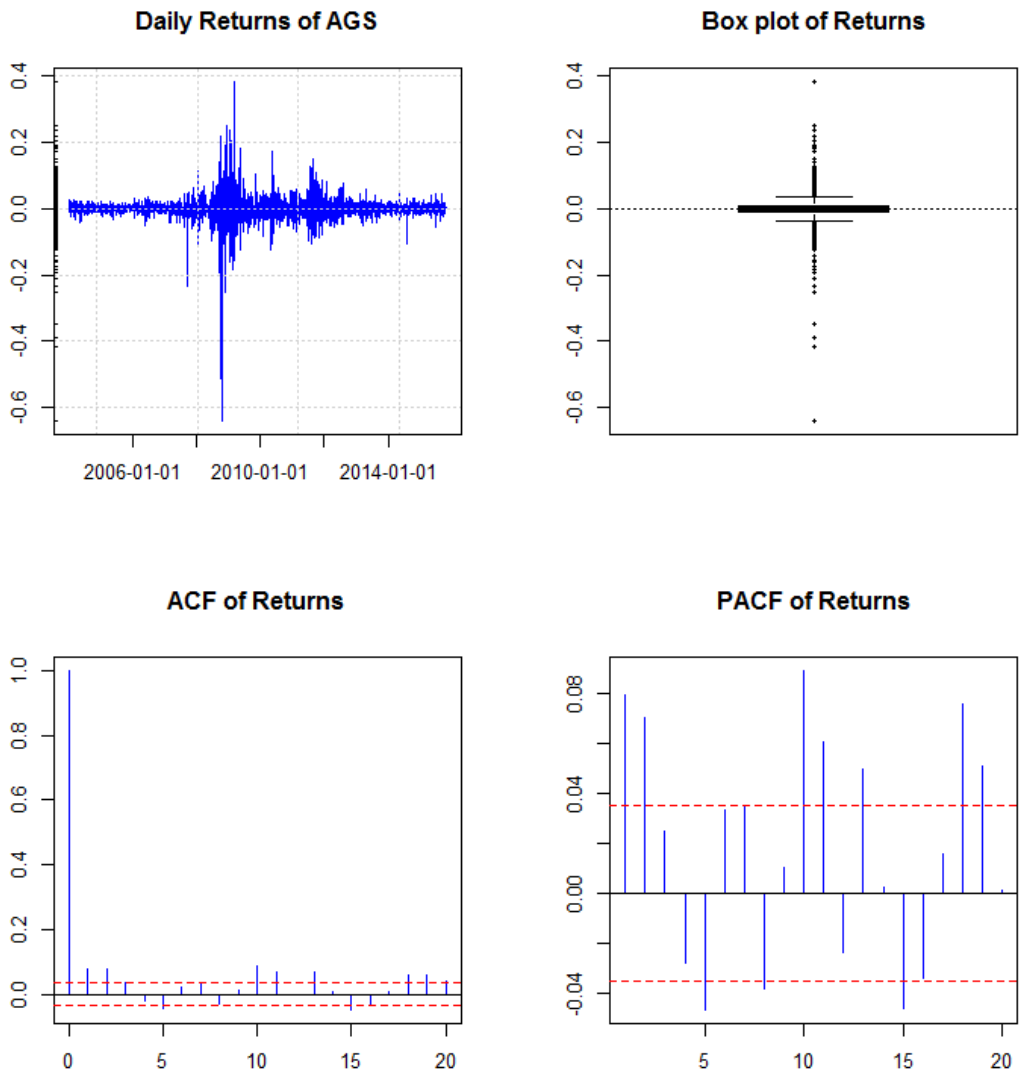

Figure 2.5: AGS - Stylistic features

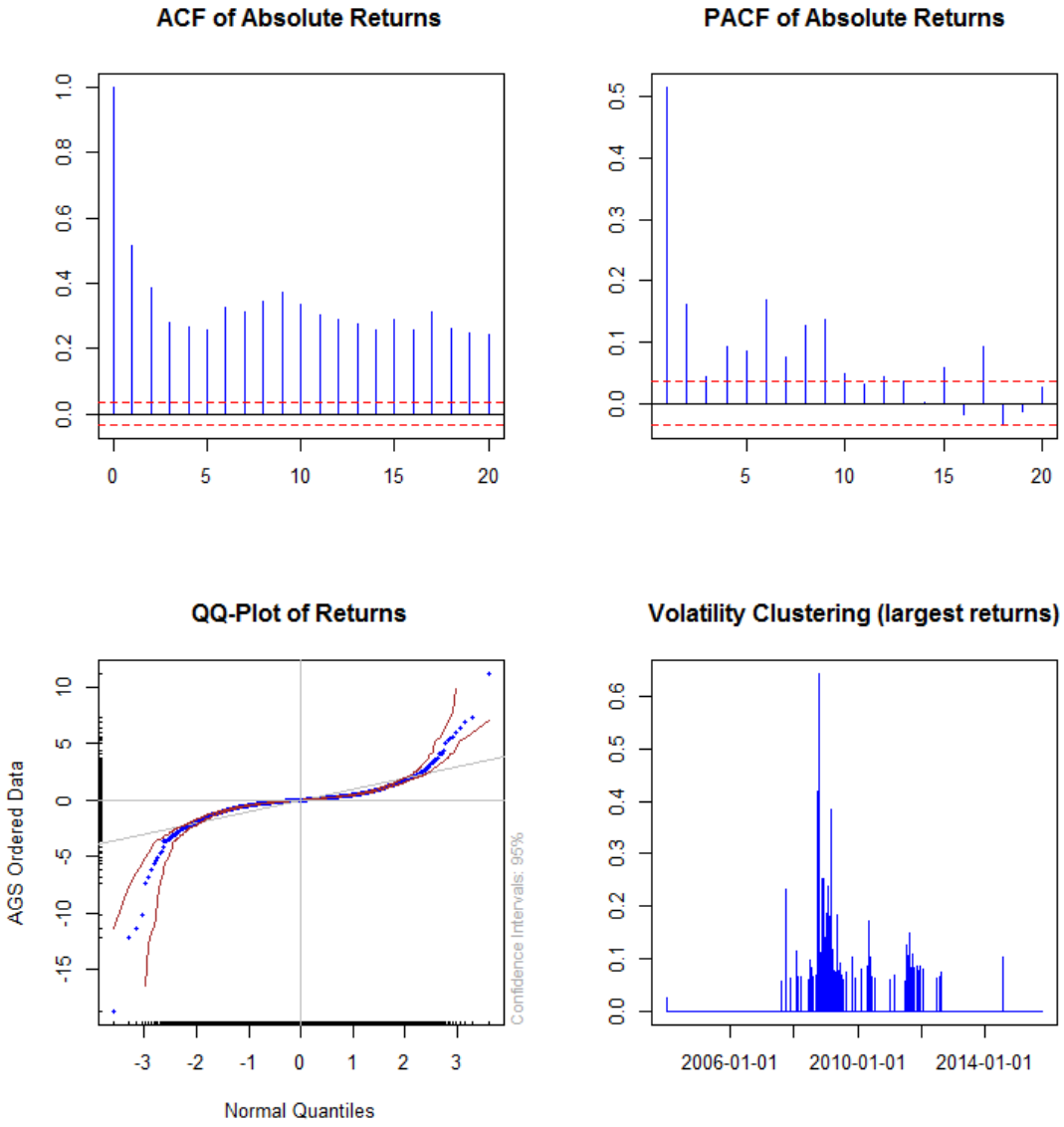

Figure 2.6: AGS - Stylistic features

2.2 Stylized facts for multivariate asset return series

The previous section presented the stylized facts for univariate financial market returns. In this section we focus our attention to the stylized facts of multivariate return series:

- The absolute (or squared) returns show high cross-correlations. This finding is similar to the univariate case.

- The absolute value of cross-correlations between return series are less pronounced. The contemporaneous correlations are in general the strongest.
- Contemporaneous correlations are not constant over time.
- Extreme observations in one return series are often accompanied by extremes in the other return series.

We illustrate the multivariate features by analyzing the XLE, XLU and XLK sector ETF asset price timeseries and their corresponding returns. The relevant timeseries are plotted in figure 2.7 and figure 2.8. These graphs clearly illustrate the co-movements in the asset prices and the simultaneous volatility clustering behavior of asset returns.

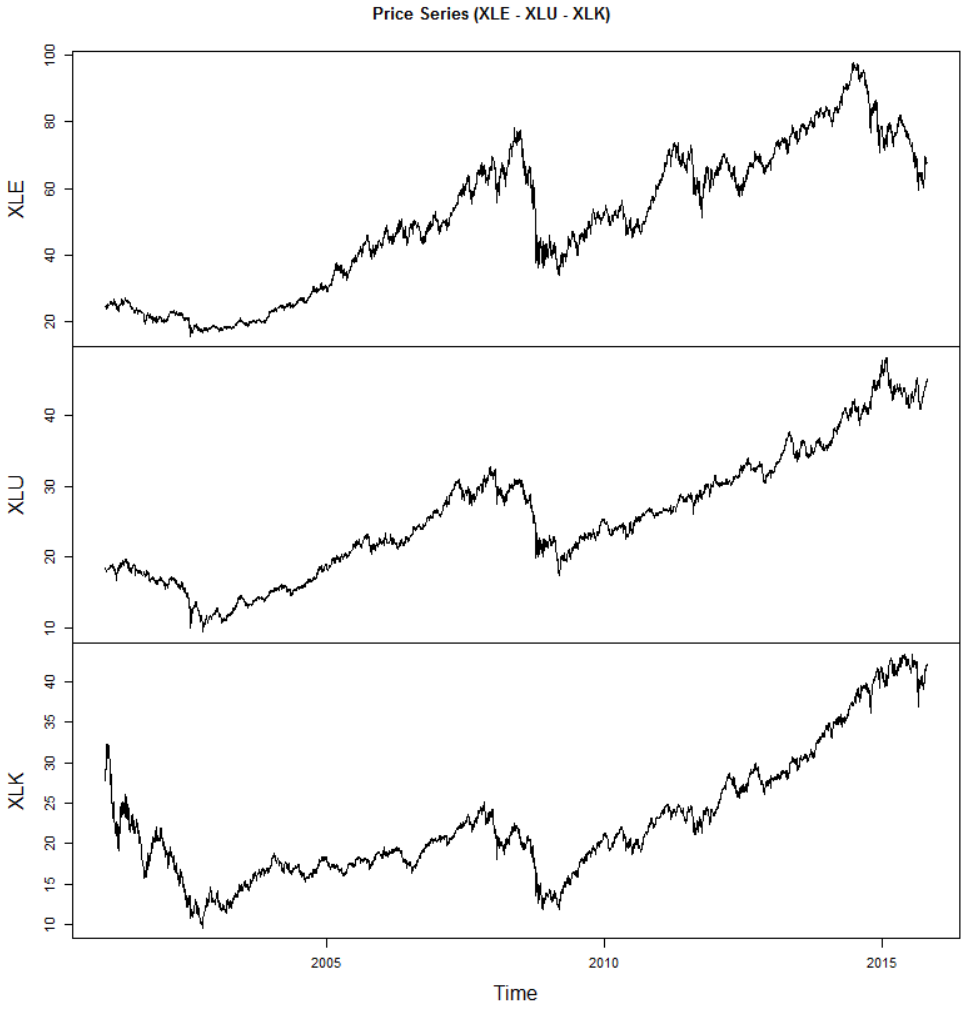

Figure 2.7: Stylistic features - Multivariate time series

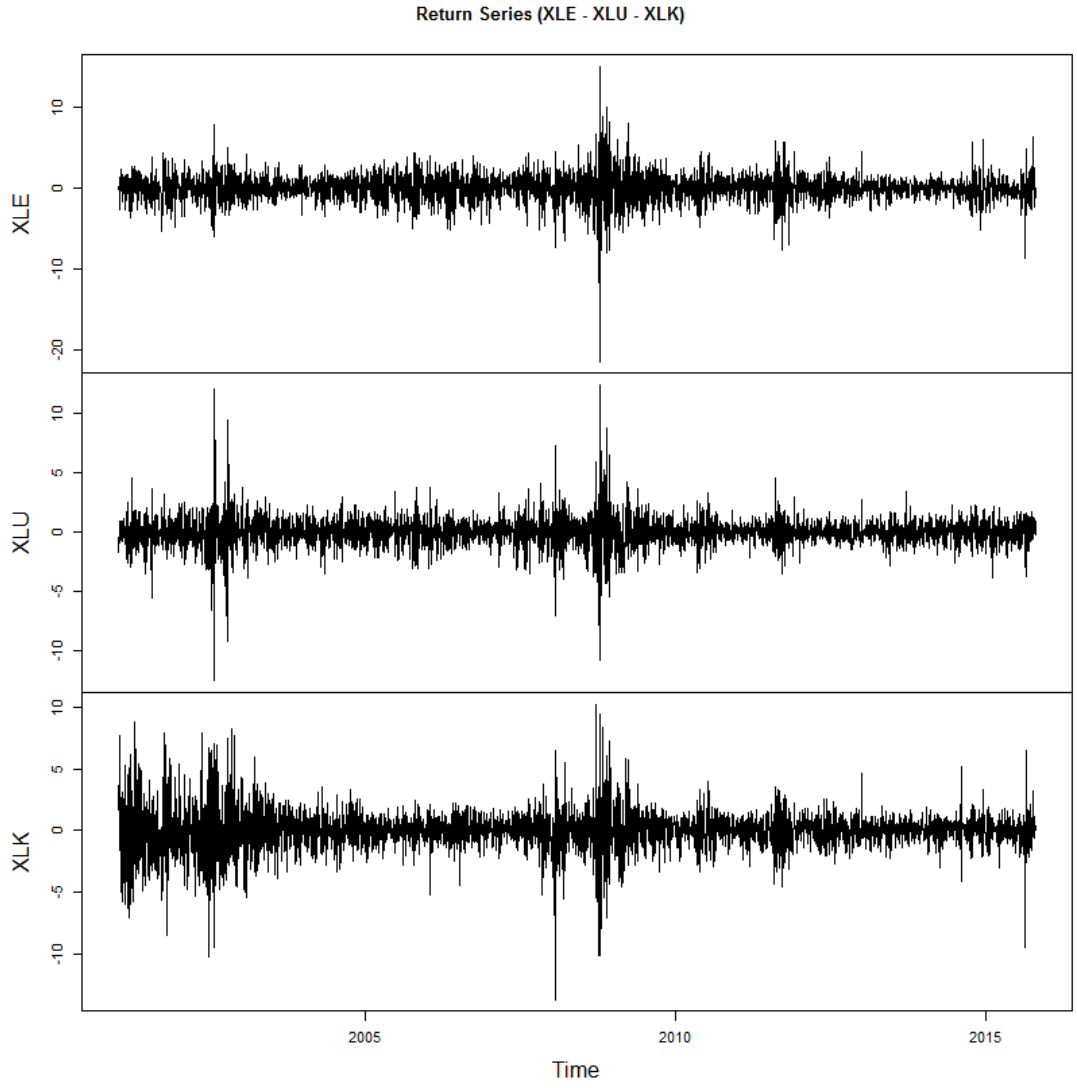

Figure 2.8: Stylistic features - Multivariate return series

Figure 2.9 displays the cross correlations of the asset returns on the left side and illustrates the cross correlations of the absolute asset returns on the right side. The graph implies that the returns are not cross correlated and taper off fairly quickly while the absolute returns are significantly cross correlated. Figure 2.10 displays the values of the asset correlations in a moving window of 250 observations. The contemporaneous correlations are clearly not stable over time and cover a wide range of values.

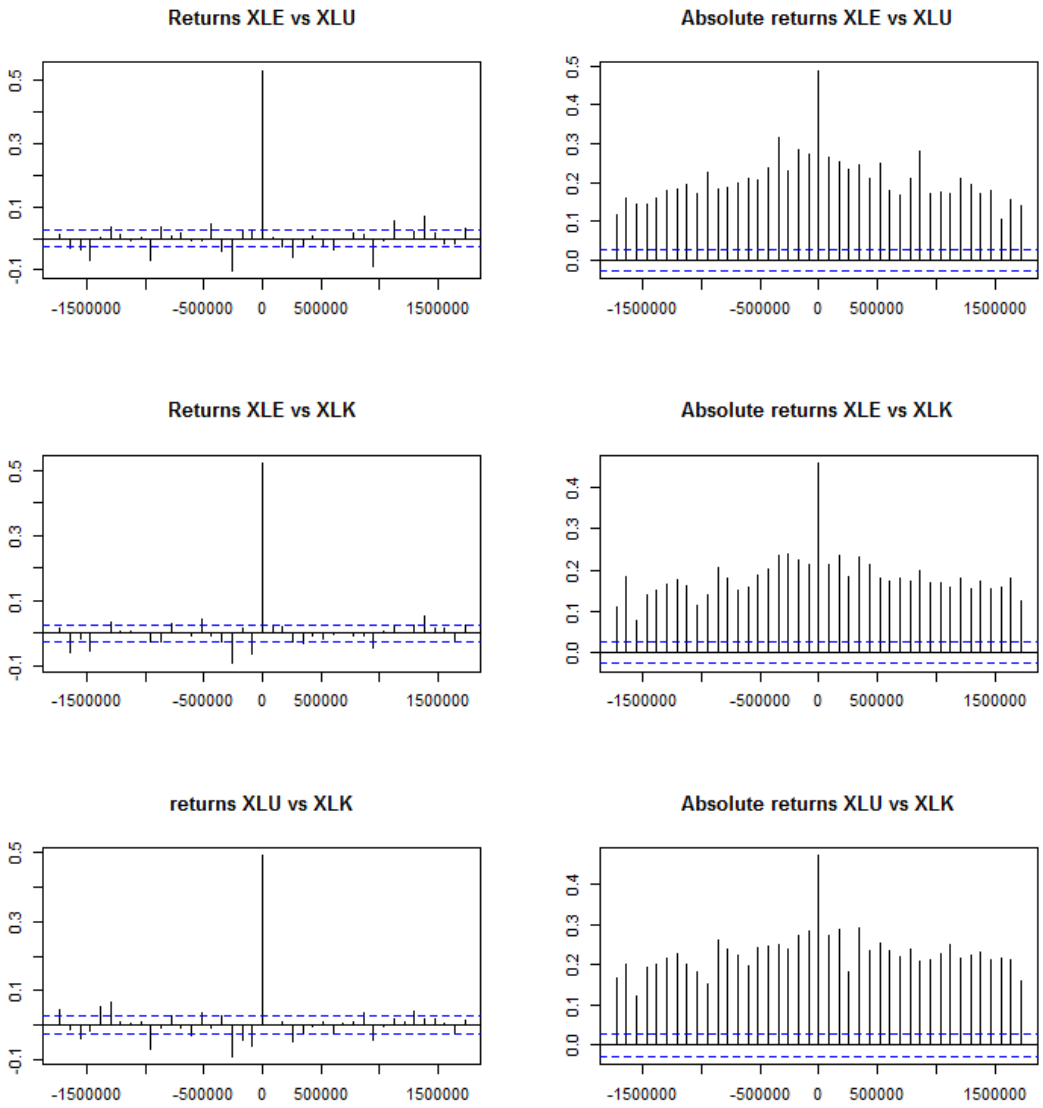

Figure 2.9: Stylistic features - Multivariate cross correlations

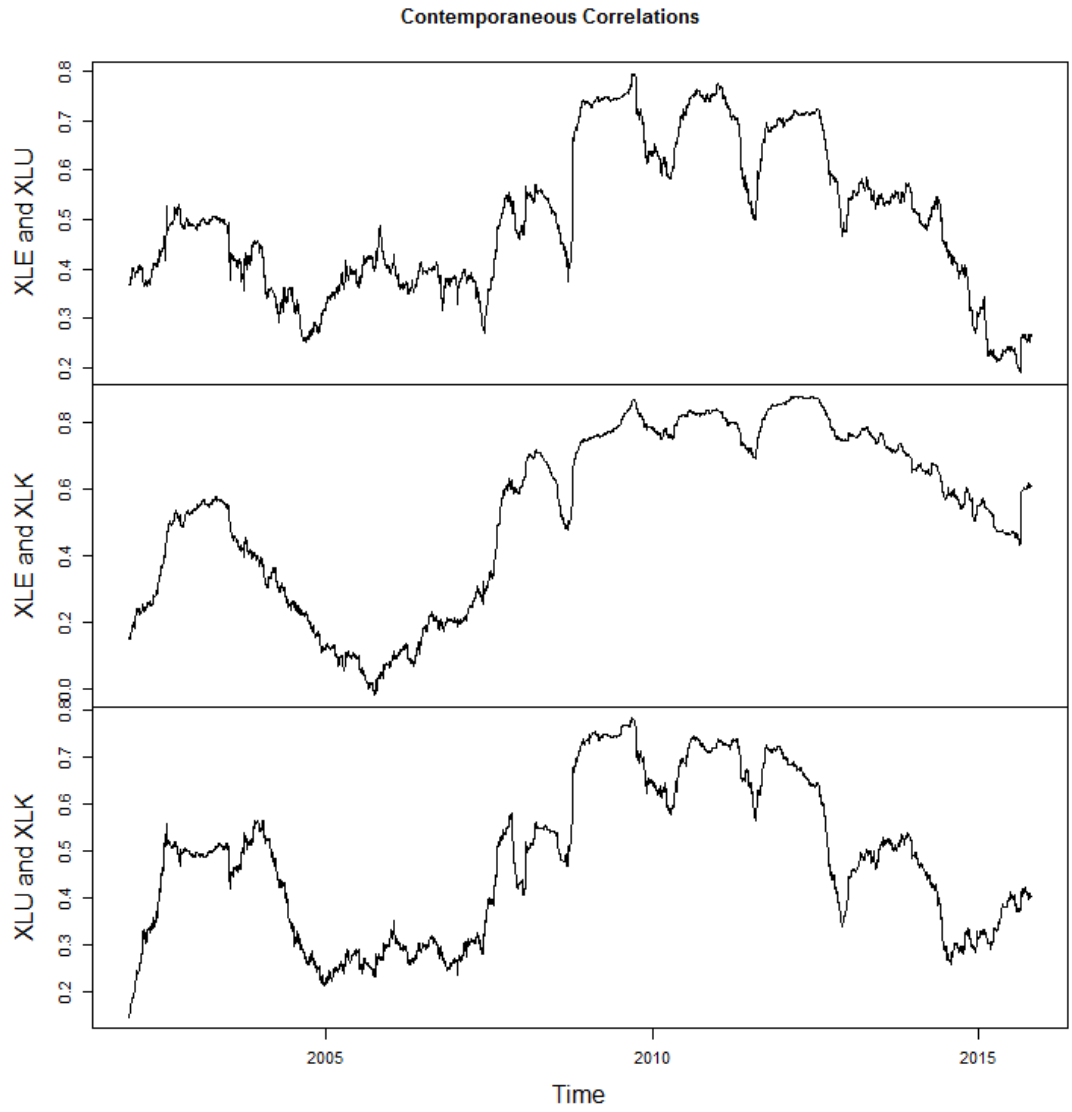

Figure 2.10: Stylistic features - Multivariate Contemporaneous correlations

2.3 Stylized facts: Implications for risk models

In the previous sections the stylized facts for both univariate and multivariate timeseries were discussed and illustrated. With respect to risk models and measures, the following requirements can be deduced[2]:

- Risk models which assume i.i.d. processes for the losses are not adequate during all market episodes.

- Risk models that are based on the normal distribution will fall short in predicting the frequency of extreme losses.
- Risk models should be able to encompass and address the different volatility regimes. This means that the derived risk measures should be adaptive to changing environments of low and high volatility.
- In the portfolio context, the employed model should be flexible enough to allow for changing dependencies between the assets; in particular, the co-movement of losses should be taken care of.

In the next chapters of this thesis we investigate the properties of a number of well known statistical models and techniques. Our main goal is to evaluate if these models are sufficiently suitable to capture the stylistic asset return properties and if they can be reliable employed in a risk management setting.

2.4 The importance of reliable risk measurement

Investors must be able to adequately measure risks during all phases of the financial business cycle. It is obvious that potential losses must be correctly anticipated during periods of financial crises and downward moving markets. On the other hand, it is equally important to correctly asses risk during market episodes that are more tranquil: Indeed, an investor could potentially jeopardize investment opportunities when being too conservative with risk.

In this section we take a closer look at the concepts of Value at Risk (VaR) and Expected Shortfall (ES) as measures of risk. We will again conclude, from a theoretical point of view, that it is imperative to take the stylistic features of asset returns into account during the modeling process in order to allow for meaningful risk evaluations.

2.4.1 Practical risk measures

In practice, the most commonly encountered risk measure is the value at risk (VaR) which was originally introduced by JP Morgan[6]. For a given confidence level $\alpha \in (0,1)$, the VaR is defined as the smallest number l such that the probability of a loss L is not higher than $1-\alpha$ for losses greater than l. This value corresponds to a quantile of the loss distribution and can be formally expressed as follows:

$$VaR_\alpha = \inf_{l\in\mathbb{R}}\{P(L > l) \leq 1-\alpha\} = \inf_{l\in\mathbb{R}}\{F_L(l) \geq \alpha\} \tag{2.1}$$

where F_L is the distribution function of the losses. However, An important flaw of the VaR entails that it is inconclusive about the size of the loss if it is greater than the value implied by the chosen confidence level. The expected shortfall (ES) risk measure, introduced by Artzner et al. (1997)[7] and Artzner (1999)[8], addresses this issue. This measure provides a value for the expected loss in the scenario that the VaR has been violated for a given level of confidence. The ES can be defined as follows:

$$ES_\alpha = \frac{1}{1-\alpha}\int_\alpha^1 q_u(F_L)du \tag{2.2}$$

where $q_u(F_L)$ is the quantile function of the loss distribution F_L. Alternatively, the ES can be expressed in terms of the VaR as follows:

$$ES_\alpha = \frac{1}{1-\alpha}\int_\alpha^1 VaR_\alpha(L)du \tag{2.3}$$

Hence, the ES can be interpreted as the average VaR in the interval $(1-\alpha, 1)$. Figure 2.11 below illustrates these concepts[2]:

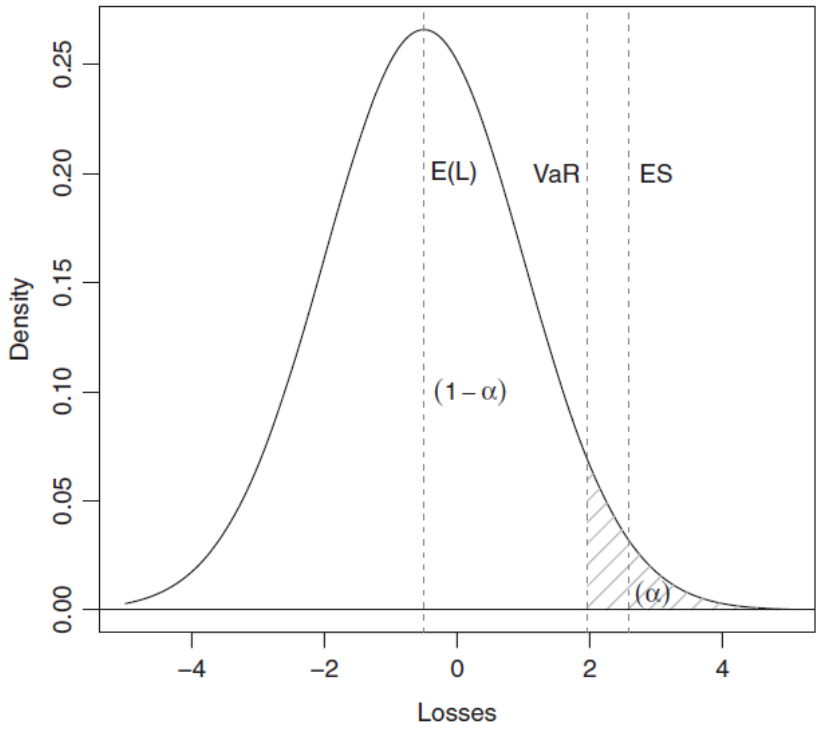

Figure 2.11: VaR and ES - Density of losses

VaR and ES can be computed based upon the empirical distribution for a given sample. Alternatively, one can obtain the required risk measure values by assuming that the losses follow a certain distribution. For example, if we assume normally distributed losses then the respective risk measures can be computed in closed form as follows:

$$VaR_\alpha = \sigma\Phi^{-1}(\alpha) - \mu \tag{2.4}$$

$$ES_\alpha = \sigma \frac{\phi(\Phi^{-1}(\alpha))}{1-\alpha} - \mu \tag{2.5}$$

However, It should be stressed that incorrect assumptions with respect to the chosen distribution can result in severe modeling errors. As we recall from the stylized features of asset returns, we can not assume normally distributed returns. For example, the empirical distribution of returns possess more probability mass in the tails than the Gaussian distribution. Hence, This stylistic fact implies that risk measures derived from the normal assumption underestimate the riskiness of a position in a financial asset.

Chapter 3

The generalized hyperbolic distribution

In this section we discuss the class of generalized hyperbolic distributions (GHD) and its special cases, the hyperbolic distribution (HYP) and the normal inverse Gaussian distribution (NIG). Our goal here is to analyze whether the distributions are capable of modelling the univariate stylistic asset return features and if the resulting models can be succesfully utilized for risk modelling purposes.

We start with a theoretical overview on the GHD distribution and subsequently calibrate our empirical data to the respective models. Next, the corresponding VaR and ES values are evaluated and compared against their empirical and normal distribution counterparts. We conclude the section with an out of sample risk assessment backtest and a statistical analysis on the results.

3.1 Theoretical overview

The Generalized Hyperbolic Distribution (GHD) was introduced in the literature by Barndorff-Nielsen (1977)[9]. Financial applications where first proposed by Eberlein and Keller (1995)[10], and were soon followed by many others. The GHD distribution owes its name to the fact that the logarithm of the density function is of hyperbolic shape (whereas the logarithmic values of the normal distribution are parabolic). The density of the GHD can be summarized as follows:

$$\begin{aligned} gh(x;\lambda,\alpha,\beta,\delta,\mu) = a(\lambda,\alpha,\beta,\delta)(\delta^2+(x-\mu)^2)^{\frac{\lambda-\frac{1}{2}}{2}} \\ \times K_{\lambda-1/2}(\alpha\sqrt{\delta^2+(x-\mu)^2})exp(\beta(x-\mu)) \end{aligned} \tag{3.1}$$

where

$$a(\lambda,\alpha,\beta,\delta) = \frac{(\alpha^2-\beta^2)^{\frac{\lambda}{2}}}{\sqrt{2\pi}\alpha^{\alpha-\frac{1}{2}}\delta^{\lambda}K_{\lambda}(\delta\sqrt{\alpha^2-\beta^2})} \tag{3.2}$$

where K_v denotes a modified third-order Bessel function with index value v. The density is defined for $x \in \mathbb{R}$ and encompasses five parameters $\lambda, \alpha, \beta, \delta, \mu$. The allowable parameter space is defined as $\lambda, \mu, \in \mathbb{R}, \delta > 0$ and $0 \leq |\beta| \leq \alpha$. The parameter$\lambda$ can be interpreted as a class-defining parameter, whereas the μ and δ are location and scale parameters. Figure 3.1 illustrates that it is possible to capture skewed distributions and/or semi long tails by using different parameter constellations. Furthermore, three reparameterizations of the GHD can be found in the literature:

$$\begin{aligned} \zeta &= \delta\sqrt{\alpha^2 - \beta^2}, \quad \rho = \beta/\alpha \\ \varepsilon &= (1+\zeta)^{-1/2}, \quad \chi = \varepsilon/\rho \\ \bar{\alpha} &= \alpha\delta, \quad \bar{\beta} = \beta\delta \end{aligned} \tag{3.3}$$

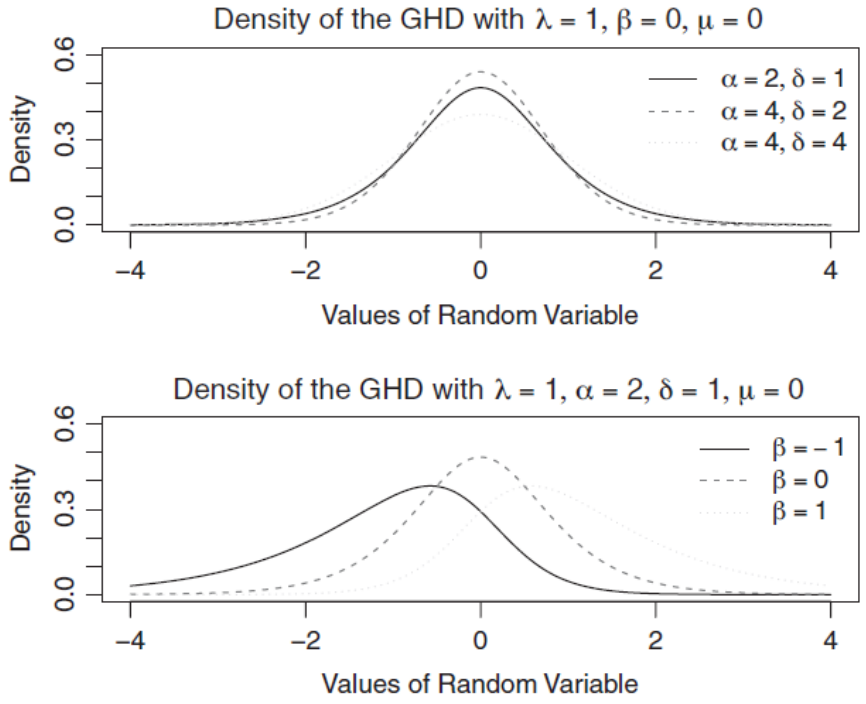

Figure 3.1: Generalized hyperbolic distribution (GHD) - Parameter constellation

It should also be noted that many other continuous distributions can be derived from the GHD: the hyperbolic, hyperboloid, normal inverse Gaussian, normal reciprocal inverse Gaussian, normal, variance gamma, Student's t, Cauchy, generalized inverse Gaussian and skewed Laplace distributions result when certain parameter restrictions are imposed. Here, we focus our attention to the hyperbolic (HYP) and the normal inverse Gaussian distribution (NIG). The HYP is a special case of the GHD that results when $\lambda = 1$.

$$hyp(x;\alpha,\beta,\delta,\mu) = \frac{\sqrt{\alpha^2-\beta^2}}{2\delta\alpha K_1(\delta\sqrt{\alpha^2-\beta^2})} exp(-\alpha\sqrt{\delta^2+(x-\mu)^2}+\beta(x-\mu)) \qquad (3.4)$$

where $x, \mu \in \mathbb{R}, 0 \leq \delta$ and $|\beta| < \alpha$. Here, the reparameterization in the form of (ε, χ) is of particular interest, since the defined range is given by $0 \leq |\chi| < \varepsilon < 1$. This relation describes the so-called shape triangle. Asymptotically, the parameters reflect the third and fourth moments of the distribution (e.g. skewness and kurtosis). The HYP can itself be viewed as a general class of distributions which encompasses the following distributions at the limit: for $\varepsilon \to 0$ a normal distribution results; for $\varepsilon \to 1$ one obtains symmetric and asymmetric Laplace distributions, for $\chi \to \pm\varepsilon$ the HYP converges to a generalized inverse Gaussian distribution and for $\chi \to 1$ an exponential distribution results. The shape triangle can therefore be used as a graphical means of assessing whether a return process can be approximated by one these distributions.

The NIG distribution results when the class-selecting parameter of the GHD is set to $\lambda = 1/2$. The density of the NIG is given by

$$nig(x;\alpha,\beta,\delta,\mu) = \frac{\alpha\delta}{\pi} exp(\delta\sqrt{\alpha^2-\beta^2}+\beta(x-\mu)) \frac{K_1(\alpha\sqrt{\delta^2+(x-\mu)^2})}{\sqrt{\delta^2+(x-\mu)^2}} \qquad (3.5)$$

where the parameter space is defined as $x, \mu \in \mathbb{R}, 0 \leq \delta$ and $0 \leq |\beta| \leq \alpha$. The unknown parameters of the GHD distribution and its special cases can be estimated by the maximum likelihood (ML) principe for any given sample. In practice, The negative log-likelihood must be minimized numerically because closed-form estimators cannot be derived.

3.2 Risk modeling application

3.2.1 Calibration of the GHD model

In this section we calibrate the parameters of the GHD, HYP and NIG distributions to the empirical return series data from SPY and AGS. Figure 3.3 illustrates the calibration results for SPY. The top left plot represents a comparison of the fitted distribution against the empirical distribution function (EDF) of the return data. Note that a Gaussian density fit was also added to the plot as a benchmark. It is immediately noticable that the normal distribution is unable to capture the excess kurtosis in the return data. In contrast, the GHD distributions manage to track the empirical distribution function rather well.

The top right graph in figure 3.3 displays a quantile-quantile plot of the theoretical model quantiles versus the empirical data. The plot illustrates that both the GHD and NIG models manage to capture the data in the tail almost equally well, while the HYP model slightly underperforms in this regard. Further analysis of diagnostic measures in figure 3.2 illustrate that the GHD model contains the highest likelihood ratio and

provides the best fit to the data while the restricted NIG model is selected as more optimal and parsimoneous by the AIC criterion.

	model	symmetric	lambda	alpha.bar	mu	sigma	gamma	aic	llh	converged	n.iter
3	NIG	FALSE	-0.5000000	0.41545880	0.10560056	1.210999	-0.07876380	11313.31	-5652.653	TRUE	145
1	ghyp	FALSE	-0.3915179	0.42094253	0.10718650	1.207700	-0.08025779	11315.19	-5652.597	TRUE	468
2	hyp	FALSE	1.0000000	0.05734685	0.09046797	1.148072	-0.06301891	11352.11	-5672.053	TRUE	177

Figure 3.2: GHD models - AIC

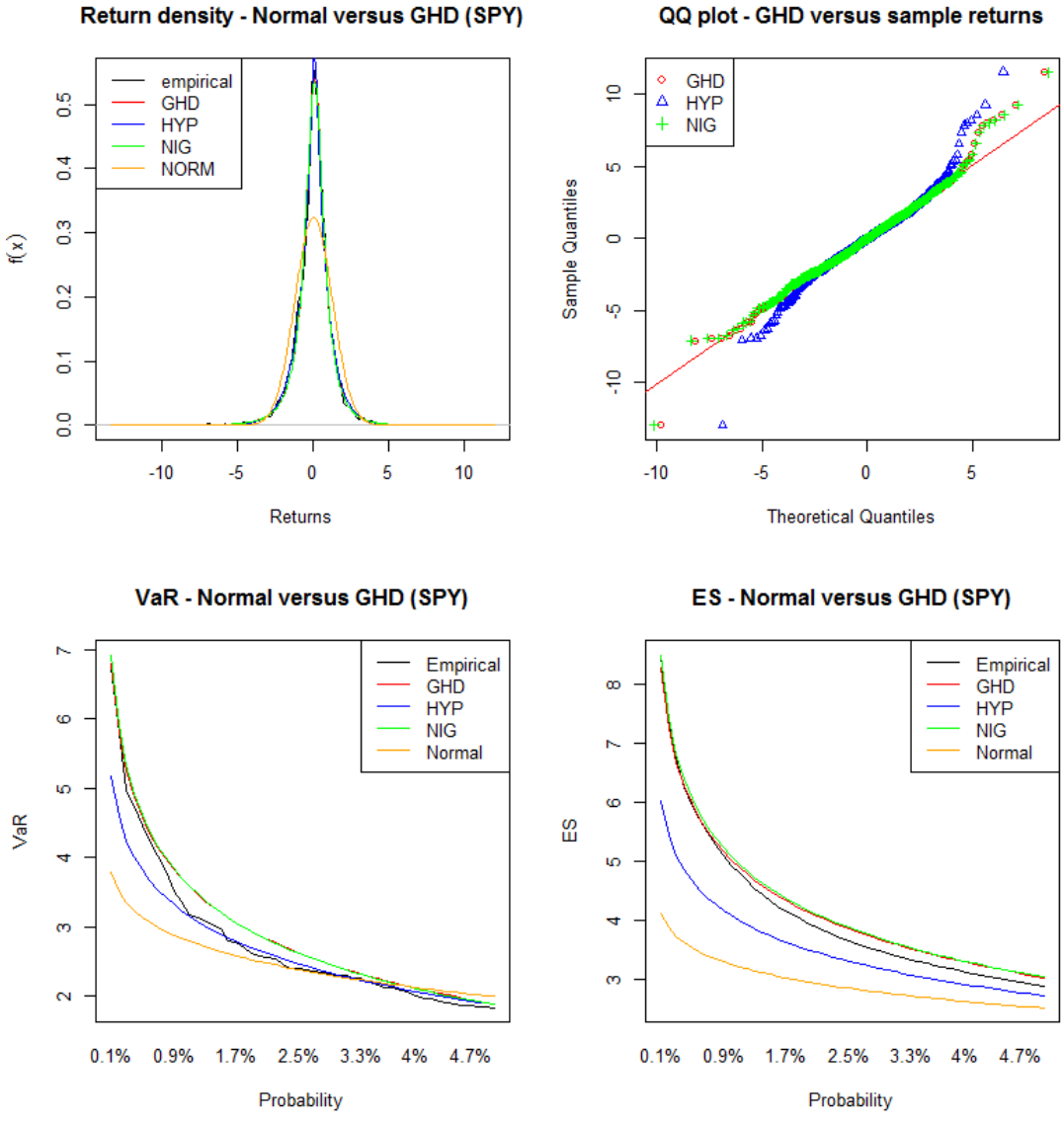

Figure 3.3: Fitting the GHD model to empirical return data (SPY)

However, a likelihood ratio test demonstrates that the hypothesis of equal explanatory power between the GHD and NIG distribution can not be rejected. For the HYP distribution on the other hand, the null hypothesis is rejected and it can be concluded that the latter model provides a less optimal fit for the empirical data.

3.2.2 Evaluation of the risk measurement forecasts

Here we investigate the behavior of the VaR and ES risk measures according to each of the models. The risk measures for SPY are calculated over a risk level span from 95% to 99.9% and the values are then compared to their empirical counterparts. Results for the VaR risk measure are illustrated in the bottom left plot of figure 3.3. Note that results for a fitted Gaussian model are provided as well. We notice that the normal distribution falls short of capturing extreme risk events while the riskiness of holding a position in the asset is overestimated for the higher confidence regions. In contrast, the GHD and NIG fit fairly well for the whole data range while HYP seems to underestimate risk in the lower confidence regions; this confirms our observations from the previous subsection.

Results for the ES risk measure are displayed in the bottom right plot of figure 3.3 and the corresponding conclusions are fairly equivalent to the VaR findings. The GHD and NIG models provide a good fit for the ES measure while both the Gaussian and normal distributions underestimate the expected losses. Note that errors are accumulated during the calculation of the ES.

The results for the AGS stock are displayed in figure 3.4 and they can be analyzed in a similar fashion. We especially note the added difficulty of the HYP distribution to capture the extremely heavy tails (and high kurtosis) of the data.

3.2.3 Out of sample backtest

In this subsection we conduct a backtest for the one day forecasted 99% VaR values of the daily returns of SPY and AGS. The backtest involves the calculation of the VaR and ES measures for both the GHD and normal distribution models in a moving window of 252 datapoints. Next, we compare the calculated risk measures with the actual realized returns that manifest themselves the following day. Results are illustrated in figure 3.5 and figure 3.6 for SPY and AGS respectively. The plots show that the VaR and ES trajectories according to the GHD model are more volatile than for the normal distribution. From an empirical point of view we would expect 1% of the one day forward returns to exceed the forecasted VaR value from the previous day: For the SPY dataset this corresponds to about 35 exceedances. Closer inspection of the SPY dataset demonstrates that there were 77 violations of the expected VaR according to the normal distribution model while only 46 exceedences were encountered for the GHD model.

In order to properly evaluate these statistics we perform conditional and unconditional Value at Risk exceedance tests[11][12] on the backtest results. The tests show that the null hypothesis of a correct amount of unconditional exceedances can not be rejected for the GHD model, while it is rejected for the Gaussian distribution model. Results for the unconditional exceedances are inconclusive. To evaluate the ES measures we

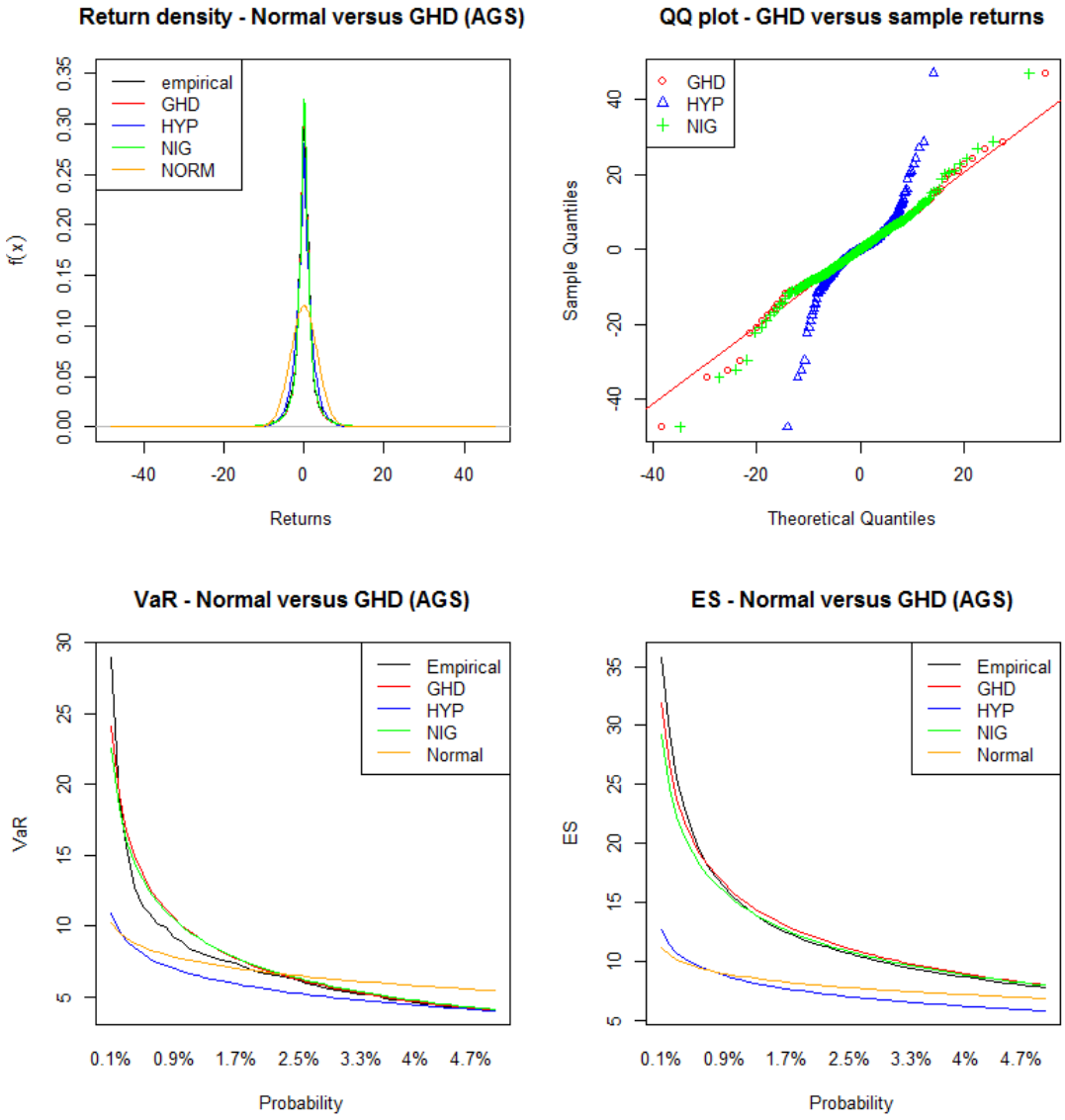

Figure 3.4: Fitting the GHD model to empirical return data (AGS)

employ the expected shortfall test of McNeil and Frey[13] which has a null hypothesis of i.i.d excess conditional shortfall with zero mean. The null hypothesis is rejected for the normal distribution but not rejected for the GHD model. Results for AGS are similar: Here, 30 exeedences were expected, while 41 violations occurred in reality. However, for this asset the null hypothesis of the expected shortfall test was rejected.

3.2.4 Performance evaluation

In general, it can be stated that the GHD distribution is sufficiently flexible to capture asset return properties. However, caution is required when using this distribution for dynamic risk modelling purposes:

- Even though the null hypothesis of the statistical VaR tests were not rejected, we encountered an overall excessive amount of expected VaR violations in our case studies.
- The distribution and properties of the return outliers in the tail might not be adequately captures by the GHD model.
- The GHD model assumes that financial market returns are identically and independently distributed. In reality this assumption is clearly violated due to the volatility clustering property of asset returns.

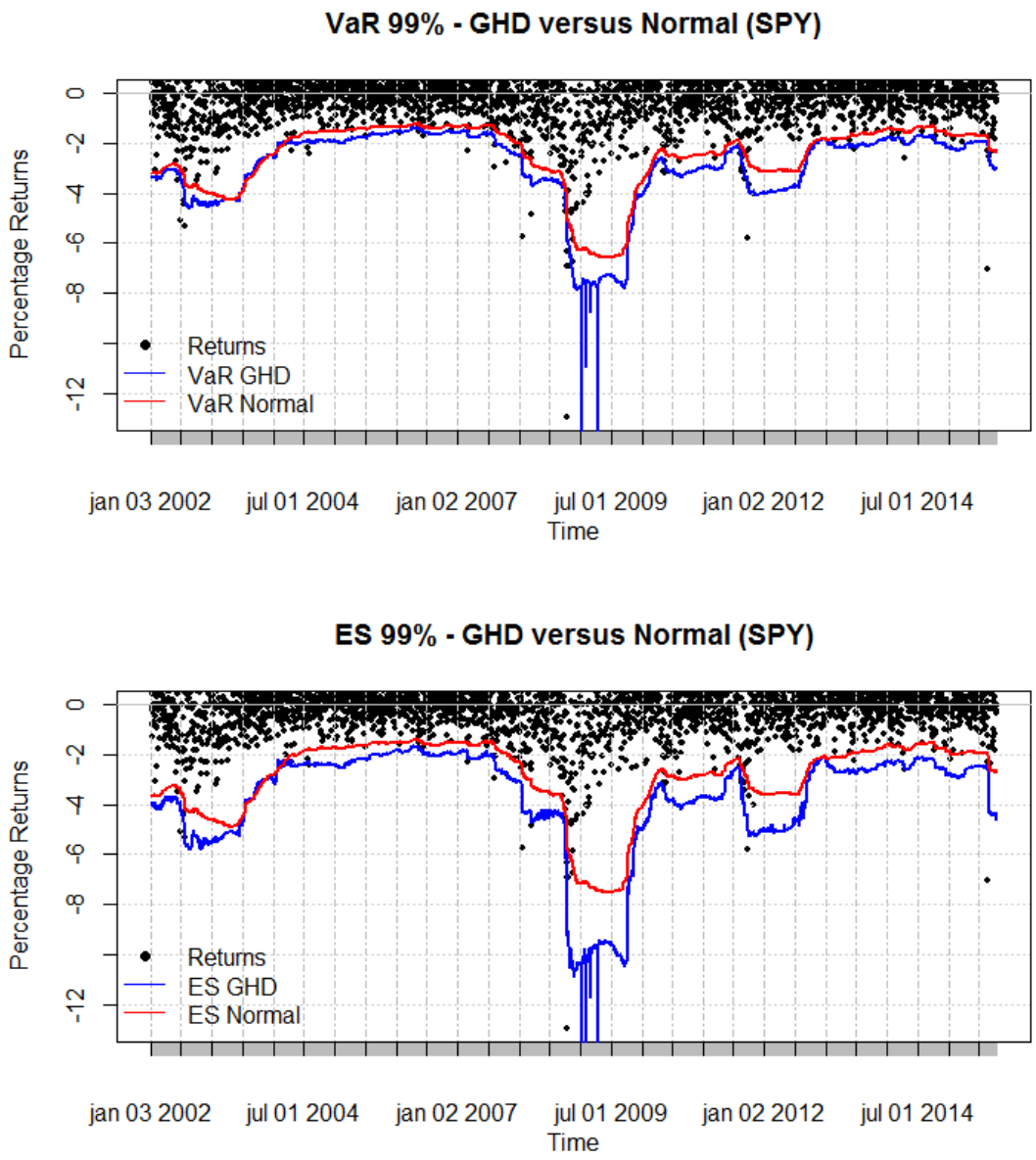

Figure 3.5: VaR and ES backtest - GHD versus Normal distribution (SPY)

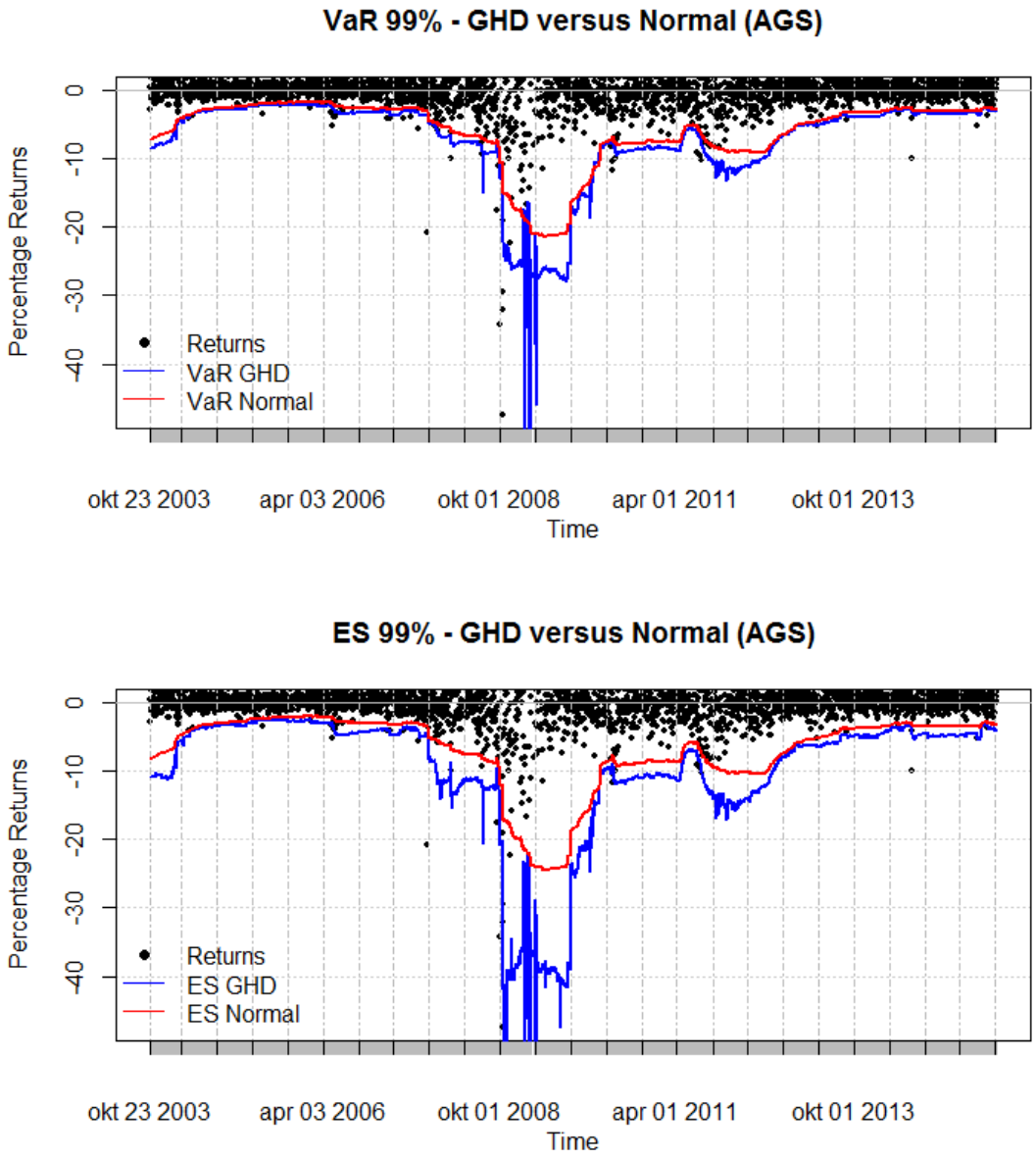

Figure 3.6: VaR and ES backtest - GHD versus Normal distribution (AGS)

Chapter 4

Extreme value theory

In subsection 2.4.1 we demonstrated that risk measures like VaR and ES are quantile values located in the left tail of a distribution. This implies that it suffices to capture only the tail probabilities adequately instead of the complete asset return distribution; This notion corresponds with the subject matter of extreme value theory (EVT).

This chapter gives a conceptual overview on the block-maxima and peaks over threshold EVT methods. For each of the methods, we illustrate practical applications geared towards financial risk modeling. For a more theoretical treatment of the subject material, we refer the reader to Coles (2001)[14] and Embrechts et al. (1997)[15].

4.1 The block maxima approach

4.1.1 Theoretical Overview

The focus of EVT is on the modelling and inference of maxima. Assume that a sequence of i.i.d. random variables $X_1, ..., X_n$ over a time span of n periods is given. Now, consider the random variables M_n, defined as follows:

$$M_n = max\{X_1, ..., X_n\} \tag{4.1}$$

We want to find out the distribution that the M_n follow, or are asymptotically best approximated by. In principle, if the distribution function for the X_i is assumed to be known then the distribution of M_n could be derived as:

$$\begin{aligned} P\{M_n\} &= P\{X_1 \leq z, ..., X_n \leq z\} \\ &= \{F(z)\}^n \end{aligned} \tag{4.2}$$

with F the distribution function of the X_i. In practice this approach is not feasible because the distribution function F is generally unknown. An alternative route would be to seek a family of distributions F^n that can be used to approximate any kind of F. Therefore, the characteristics and properties of F^n for $n \to \infty$ need to be investigated. However, this asymptotic reasoning would imply that the values of the distribution

function for z less than z_+ approach zero, whereby z_+ denotes the upper right point. Put differently, the mass of the distribution would collapse over the point z_+. This artifact can be circumvented by a linear transformation $M_n^* = \frac{M_n - b_n}{a_n}$ where $a_n > 0$ and b_n are sequences of constants. The purpose of these constants is to straighten out M_n such that the probability mass would not collapse over a single point. Under the assumption that the sequences a_n and b_n exist, it can be shown that the following probability expression converges to a non-degenerate distribution $G(z)$:

$$P\left\{ M_n^* = \frac{M_n) - b_n}{a_n} \leq z \right\} \rightarrow G(z) \text{ for } n \rightarrow \infty \tag{4.3}$$

$G(z)$ represents a non-degenerate distribution, which belongs to one of the following distribution families: Gumbel, Fréchet or Weibull. These distributions can be incorporated into the generalized extreme value (GEV) distribution.

$$G_z = exp\{-1 \cdot (1 + \varepsilon \frac{(z-\mu)}{\sigma})^{-1/\varepsilon}\} \tag{4.4}$$

The GEV is a three-parameter distribution where μ is the location, σ the scale and ε the shape parameter. For the limit $\varepsilon \rightarrow 0$ the Gumbel distribution is obtained, for $\varepsilon > 0$ we get the Fréchet, and for $\varepsilon < 0$ the Weibull. The Weibull has a finite right point, whereas z_+ is infinity for the other two distributions. The density is exponential in the case of Gumbel and polynomial for the Fréchet distribution. Hence, the characteristics and properties of the GEV can be deduced from the value of the shape parameter.

4.1.2 Risk modeling application

GEV calibration

In this subsection we convert the daily returns of SPY to positive loss figures and subsequently calibrate the GEV distribution to the data by using a 50 day block size. Figure 4.1 illustrates the 'extreme datapoints' that are utilized during the calibration process. Note that this graph displays clusters of lower and higher volatility block-maxima values, which implies that the assumption of identically distributed block maxima is violated.

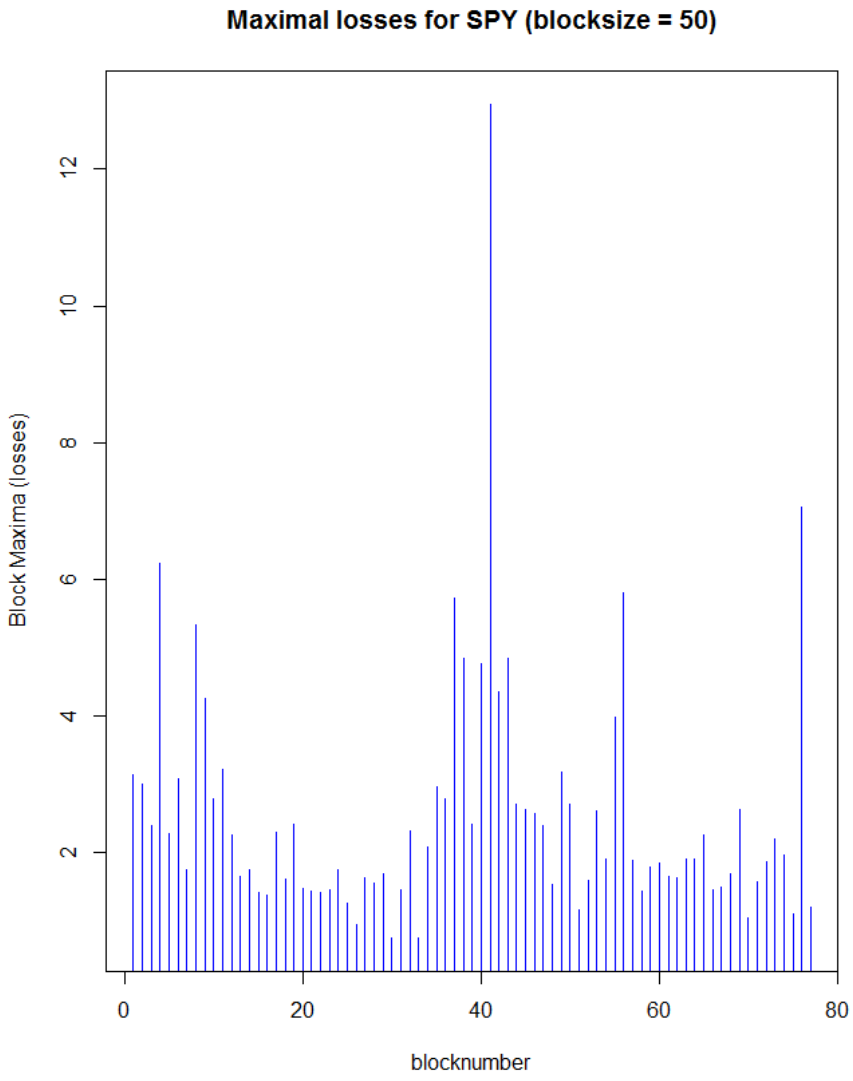

Figure 4.1: 50 day block maxima - SPY)

The ML estimation results are provided in Table 4.1; All coefficients are significantly different from zero. The estimate of the shape parameter ε implies that the GEV is of the fréchet type and hence contains heavy tails and non-finite losses.

GEV	ε	σ	μ
Estimate	0.31	0.77	1.76
Standard Error	0.09	0.08	0.1

Table 4.1: GEV parameter calibration - SPY

Figure 4.2 further illustrates the results of the calibration process. As indicated by the probability and quantile-quantile plots, data points in the far right tail are not captured adequately well by this model specification. This can be attributed to the relatively small losses witnessed during the beginning and the end of the sample period, in comparison to the more extreme values during the sub-prime mortgage crisis period. This artifact shows up in the return level plot as well. For data points in the far right tail the estimated return levels fall short compared to the empirical levels. However, they stay within the 95% confidence bands for the most part.

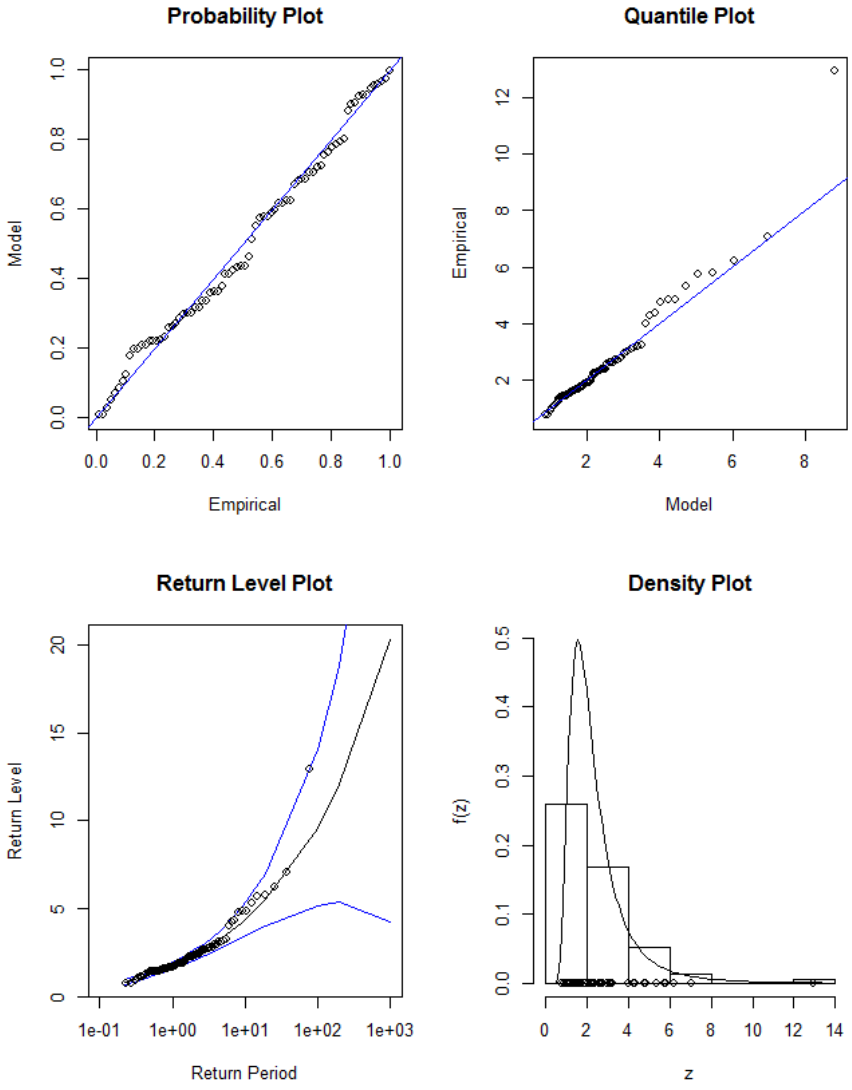

Figure 4.2: Diagnostic plots for fitted GEV model (SPY)

Figure 4.3 illustrates the two year profile log-likelihood for the return level in the

upper panel and for the shape parameter in the lower panel; Point estimates are shown together with their 95% confidence regions. The plot indicates that a daily loss as high as 4.2% would be observed about once every two years, which corresponds to 7 occurances over the complete 14 year time period. However, in practice 25 such events have manifested themselves. The maximum observed loss of SPY occurred on october 10th 2008 and entailed a daily loss of 12.95%. According to our model such an extreme loss only occurs about once every 49 years.

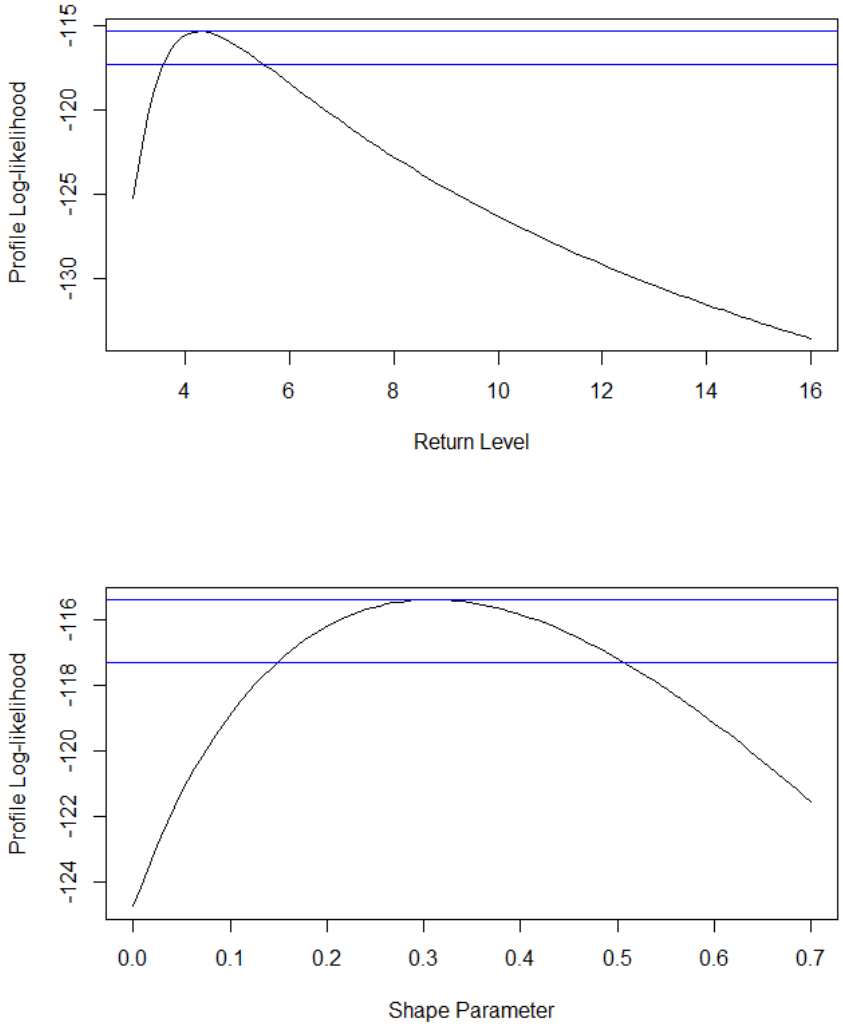

Figure 4.3: 2 year protfile log-Likelihood plots for fitted GEV model)

Performance Evaluation

As we have illustrated in this subsection, multiple problems manifest themselves when applying the block maxima approach to financial time series data. Often times, the unknown distribution parameters are estimated with great uncertainty as a result of insufficient data history. Furthermore, not all observations that can be considered extreme are exploited during the calibration process. Indeed, multiple potential outliers from the same block are potentially ignored. Additionally, data points during tranquil periods are selected as block maxima when they are in fact not extreme datapoints. The latter two issues manifest themselves as a direct result of the volatility clustering feature of univariate asset returns. It can be concluded that the block-maxima approach fails to adequately account for the stylistic asset return properties. Hence, risk measurement tests are not conducted for this model.

4.2 The peaks-over-threshold-approach

4.2.1 Theoretical Overview

The peaks-over-threshold-approach aims to circumvent the issues encountered by the block-maxima approach. All observations above a certain threshold are now considered extreme observations. This concept can be summarized for a given threshold u by the following probability expression:

$$P\{X > u + y | X > u\} = \frac{1 - F(u + y)}{1 - F(u)}, \quad y > 0 \tag{4.5}$$

Once again, in practice,the distribution function F is generally unknown. Hence, similarly to the derivation of the GEV, one needs an approximative distribution for sufficiently large threshold values. It can be shown that the exceedances $(X - u)$ are distributed according to the generalized Pareto distribution (GPD):

$$H(y) = 1 - (1 + \frac{\varepsilon y}{\tilde{\sigma}})^{-1/\varepsilon} \tag{4.6}$$

Parameters of the GDP can be estimated by applying the ML principe but difficulty arises when selecting an adequate threshold value u. If the threshold value is chosen too small then the GDP approximation will be violated. On the other hand, if the value is chosen too large then the sample size might be insufficient to yield reliable estimates. In practice we can determine an adequate threshold value by means of a residual life (MRL) plot. Such a plot is based on the expected value of the GPD: $E(Y) = \sigma(1 - \varepsilon)$. For a given range of thresholds u_0 the conditional expected values.

$$E(X - u_0 | X > u_0) = \frac{\sigma_{u_0}}{1 - \varepsilon} = \frac{\sigma_u}{1 - \varepsilon} = \frac{\sigma_{u_0} + \varepsilon u}{1 - \varepsilon} \tag{4.7}$$

are plotted against u. This equation is linear with respect to the threshold u:

$$\left\{(u, \frac{1}{n_u}\sum_{i=1}^{n_u}(x_i - u)) : u < x_{max}\right\} \tag{4.8}$$

Hence, a suitable value for u is given when this line starts to become linear. Note that confidence bands can also be calculated according to the normal distribution function, due to the central limit theorem.

4.2.2 Risk modeling application

GPD calibration

Figure 4.4 displays an MRL plot for the losses of SPY. It seems fairly hard to infer a correct threshold u from this graph so for illustration purposes we choose the 99th quatile value of the empirical data as our threshold: This corresponds to a value of 3.37%

Figure 4.5 illustrates the GPD calibration results. The upper panels show the fitted excess distribution and a tail plot. Both indicate a good fit of the GPD to the exceedances. The lower panels display the residuals with a fitted ordinary least-squares on the left and a quantile-quantile plot on the right. Neither plot gives cause for concerns because the OLS line stays fairly flat and in the quantile-quantile plot the plotted points do not deviate much from the diagonal.

Performance evaluation

We conclude that GPD model captures the tail distrbitution of asset returns in a satisfactory manner and worst case risk metrics -such as VaR and ES- can hence be derived from this tail distribution. However, calibration of asset return data to the GPD suffers from the same shortcommings previously mentioned during our GHD exposition. Asset returns are assumed to be i.i.d and dynamic autocorrelation / volatility clustering properties are not taken into account. Strong caution is advised when performing out of sample risk forecasts. Recent market conditions should manually be taken into consideration to assess the reliability of the forecasts.

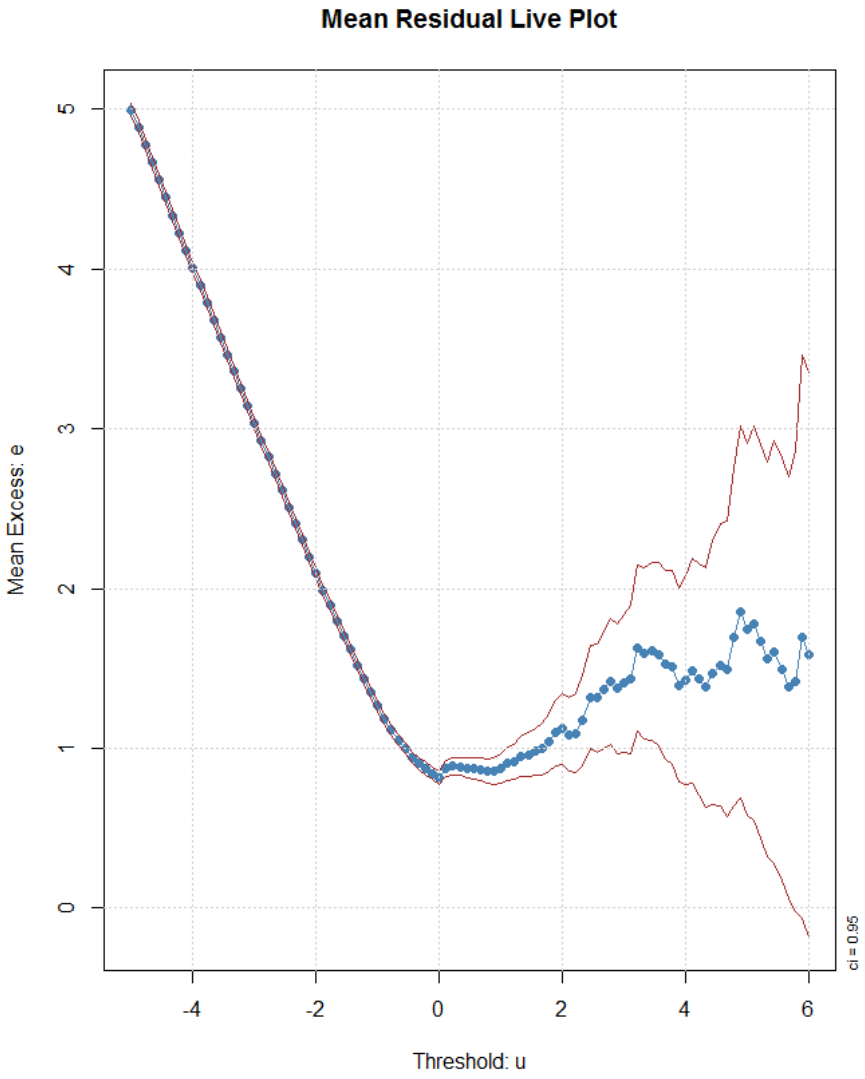

Figure 4.4: MRL plot for SPY losses

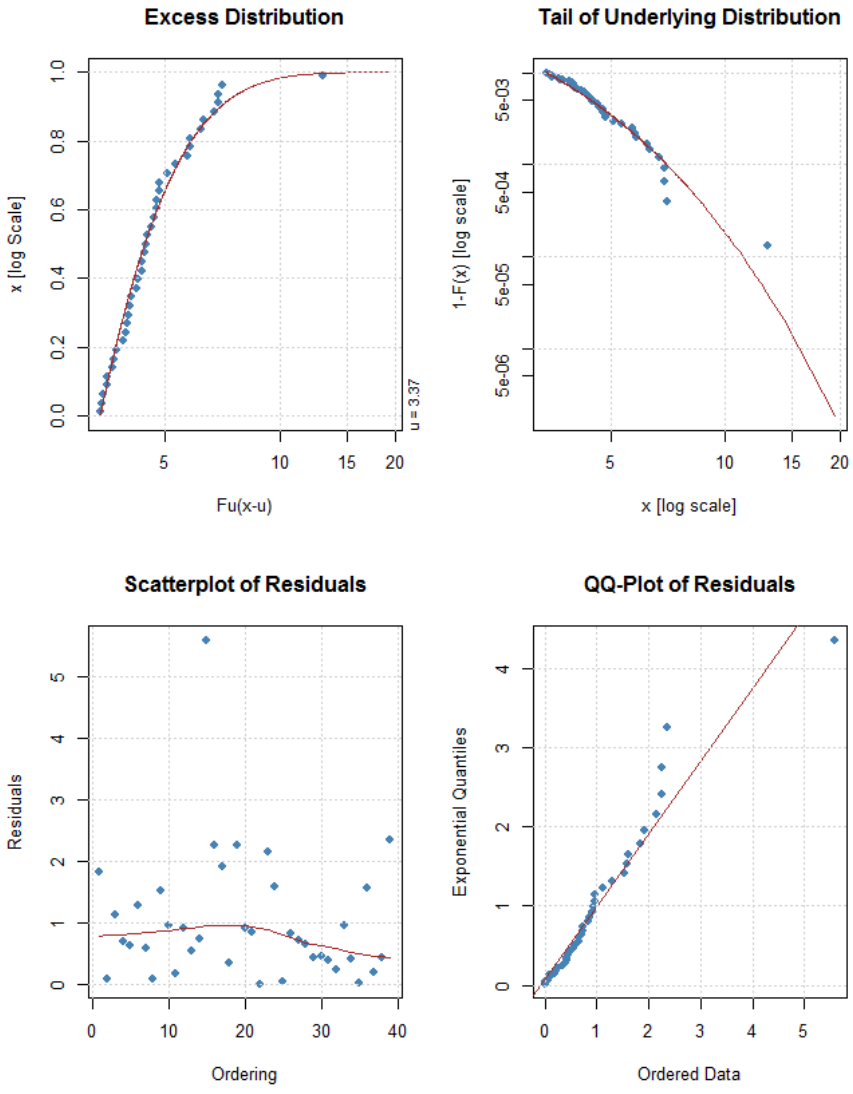

Figure 4.5: MRL plot for SPY losses

Chapter 5

Modeling volatility

The models from the previous sections assume that financial market returns are identically and independently distributed. Hence, risk measures associated to these models are unconditional in the sense that they do not depend on any prior information. However, given the volatility clustering properties of asset returns, this unconditional i.i.d assumption is clearly violated. In this chapter we introduce the class of autocorrelated conditional heteroscedastic (ARCH) models that are able to account for this volatility clustering property. We will then demonstrate how these models can be utilized to succesfully deduct conditional risk measures.

5.1 The ARCH model and its extensions

ARCH models were first introduced in the literature by Engle (1982)[16] and have since been modified and extended in several ways. The articles by Engle and Bollerslev (1986)[17], Bollerslev et al. (1992)[18] and Bera and Higgins (1993)[19] provide an overview of the most important model extensions. Our focus here will be on their application towards financial modeling and risk management.

The starting point of an ARCH model can be expressed as a linear regression expectations equation. However, the model differs from classical linear regression with respect to the assumption of i.i.d normally distributed errors:

$$y_t = x_t'\beta + \varepsilon_t, \tag{5.1}$$

$$\varepsilon = \eta_t\sqrt{h_t}, \tag{5.2}$$

$$\eta_t \sim \mathcal{D}_\nu(0,1), \tag{5.3}$$

where η_t denotes a random variable with distribution $\mathcal{D}$ with expected value zero, unit variance and additional parameters that are contained in ν. Note that this specification allows distributions with excess kurtosis and/or skewness to be interspersed inside the model. In fact, we can employ any conditional distribution that we like: For example, the GHD type distributions from chapter 3 might come up as a good candidate. The

second building block for the ARCH model is the variance equation, which can be defined as follows:

$$h_t = \alpha_0 + \alpha_1 \varepsilon_{t-1}^2 + ... + \alpha_q \varepsilon_{t-q}^2 \tag{5.4}$$

where $\alpha_0 > 0$ and $\alpha_i \geq 0, i = 1, ..., q$ such that the variance remains strictly positive. Hence, the conditional variance is explained by the errors from the previous periods. If these errors are large in absolute value then a large value for the conditional variance results, and vice versa.

The most well known extension to this simple ARCH model can be found in the Generalized ARCH(p,q) specification (GARCH), where lagged endogenous variables are also included inside the variance equation:

$$h_t = \alpha_0 + \alpha_1 \varepsilon_{t-1}^2 + ... + \alpha_q \varepsilon_{t-q}^2 + \beta_1 h_{t-1} + ... + \beta_p h_{t-p} \tag{5.5}$$

with $\alpha_0 > 0$ and $\alpha_i \geq 0, i = 1, ..., q$ and $\beta_i \geq 0$ for $j = 1, ..., p$, such that the conditional variance process again remains strictly positive. The advantage of this model is that it is equivalent to an ARCH model with an infinite number of lags (if the roots of the lag polynomial $1 - \beta(z)$ lie outside the unit circle). Hence, a more parsimonious specification is possible when using GARCH models.

It is important to note that in the (G)ARCH specifications the sign of the shock does not have an impact on the conditional variance because the past errors enter as squares into the variance equation. However, in a financial asset return context asymmetric effects between volatility and past returns can be observed empirically, in particular when equity returns are investigated. The class of exponential GARCH (EGARCH) models allows us to model such asymmetries by defining the variance equation as follows:

$$log(h_t) = \alpha_0 + \sum_{i=1}^{q} \alpha_i g(\eta_{t-i}) + \sum_{j=1}^{p} \beta_j log(h_{t-j}), \tag{5.6}$$

$$g(\eta_t) = \theta \eta_t + \gamma \Big[|\eta_t| - E(|\eta_t|) \Big] \tag{5.7}$$

Using this specification, there is no need for non-negativity constraints on the parameter space because $h_t = exp(.)$ will always be positive. Furthermore, the impact of the error variance is piecewise linear and takes a value of $\alpha_i(\theta + \gamma)$ for a positive shock and $\alpha_i(\theta - \gamma)$ for a negative shock. Hence, the contemporaneous conditional variance is dependant on the sign of the past errors. We also note that greater variations of the variable η_t from its expected value results in higher values of the function $g(\eta_t)$ and hence of the log-value for the conditional variance.

5.2 Risk modeling application

5.2.1 ARMA-EGARCH: Risk measurement forecasting

In this section we evaluate the risk forecasting power of an ARMA($p1$,$q1$)-EGARCH($p2$,$q2$) model by conducting an out of sample risk forecasting backtest. More concretely, we can write the ARMA-EGARCH model specification as follows:

$$X_t = \mu_t + \varepsilon_t, \tag{5.8}$$

$$\mu_t = \mu + \sum_{i=1}^{p_1} \phi(X_{t-i} - \mu) + \sum_{j=1}^{q_1} \theta_j \varepsilon_{t-j}, \tag{5.9}$$

$$\varepsilon_t = h_t \mathcal{Z}_t, \quad \mathcal{Z}_t \sim \mathcal{D}_v(0,1), \tag{5.10}$$

$$log(h_t) = \alpha_0 + \sum_{i=1}^{q_2} \alpha_i g(\eta_{t-i}) + \sum_{j=1}^{p_2} \beta_j log(h_{t-j}), \tag{5.11}$$

$$g(\eta_t) = \theta\eta_t + \gamma\Big[|\eta_t| - E(|\eta_t|)\Big] \tag{5.12}$$

During the backtest we fit the model to the historical data in a moving window of 500 data points. We only recalibrate the model every 10 days for performance reasons: Here, we use an ARMA(0,0)-Egarch(1,1) specification and employ a standardized skewed t distribution as $\mathcal{D}_v(0,1)$. Estimates for the unknown model parameters can be obtained by the ML principle. Next, the calibrated model is utilized to make one day forecasts of both $\mu(=0)$ and σ in a sliding window. The fitted standardized conditional distribution and the next days parameter forecasts are subsequently utilized to calculate the VaR and ES forecasts. Results are then compared against the realized returns and they are summarized in table 5.1.

Asset	E[Exceedances]	Actual Exc.	Conditional VaRtest	ES test
SPY	33	42	Fail to Reject	Fail to Reject
ACKB	25	34	Fail to Reject	Fail to Reject

Table 5.1: Egarch VaR / ES forecasting - results

The graphs in figure 5.1 and figure 5.2 further illustrate the results. From these graphs we conclude that the spikes of the daily losses are adequately captured and that the risk measures decrease rapidly during the more tranquil periods. Furthermore, a VaRtest shows that the null hypothesis of a correct amount of conditional exceedances can not be rejected.

5.2.2 Performance Evaluation

In this section, we demonstrated that EGARCH models manage to succesfully incorporate the volatility clustering properties of asset returns while also taking the other

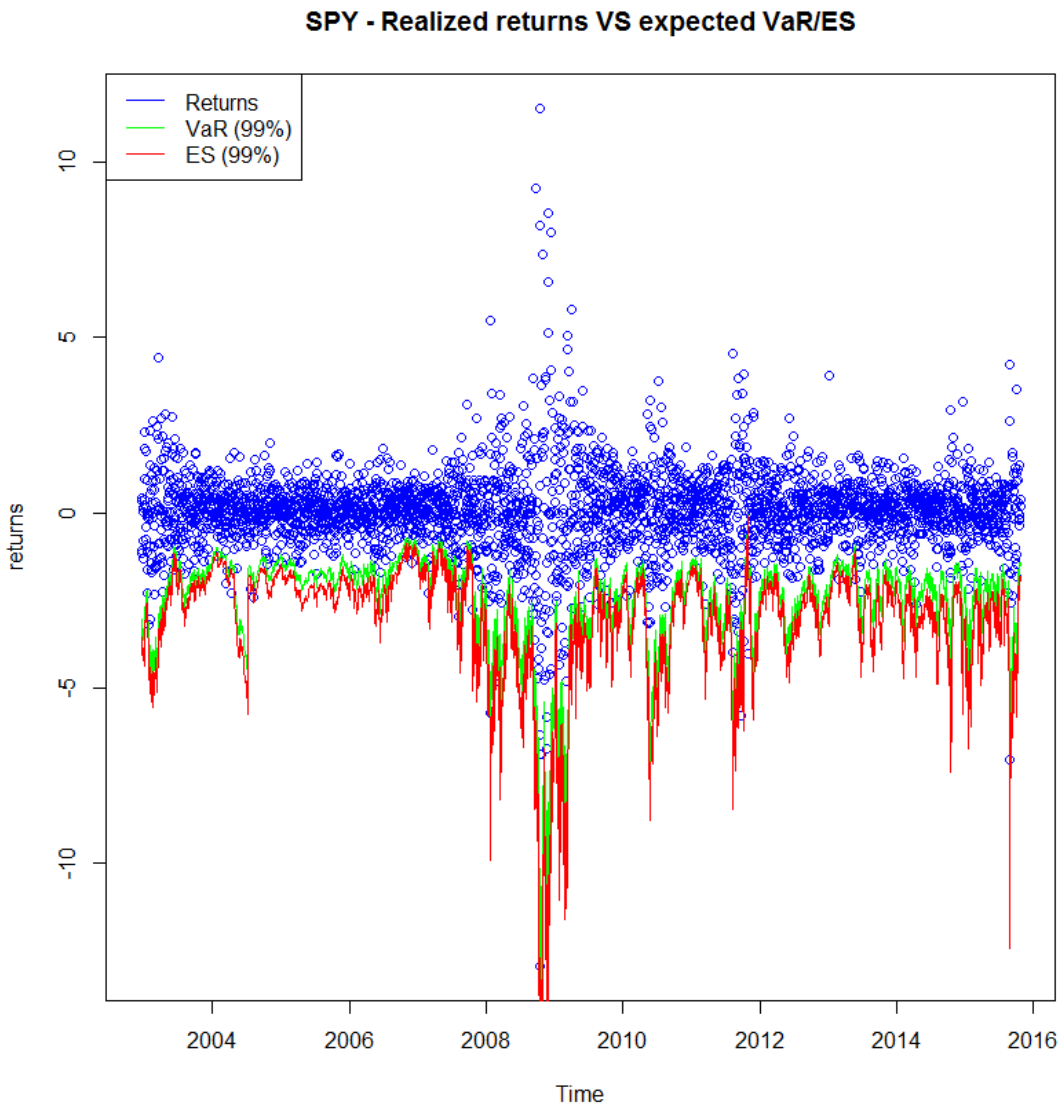

Figure 5.1: Egarch - expected VaR / ES (SPY)

stylistic properties of asset returns into account. EGARCH models take past market conditions into consideration and they circumvent the problems that were encountered during previous evaluations of the GHD and GPD models. Hence, EGARCH models are well suited to perform out of sample risk measurement forecasts.

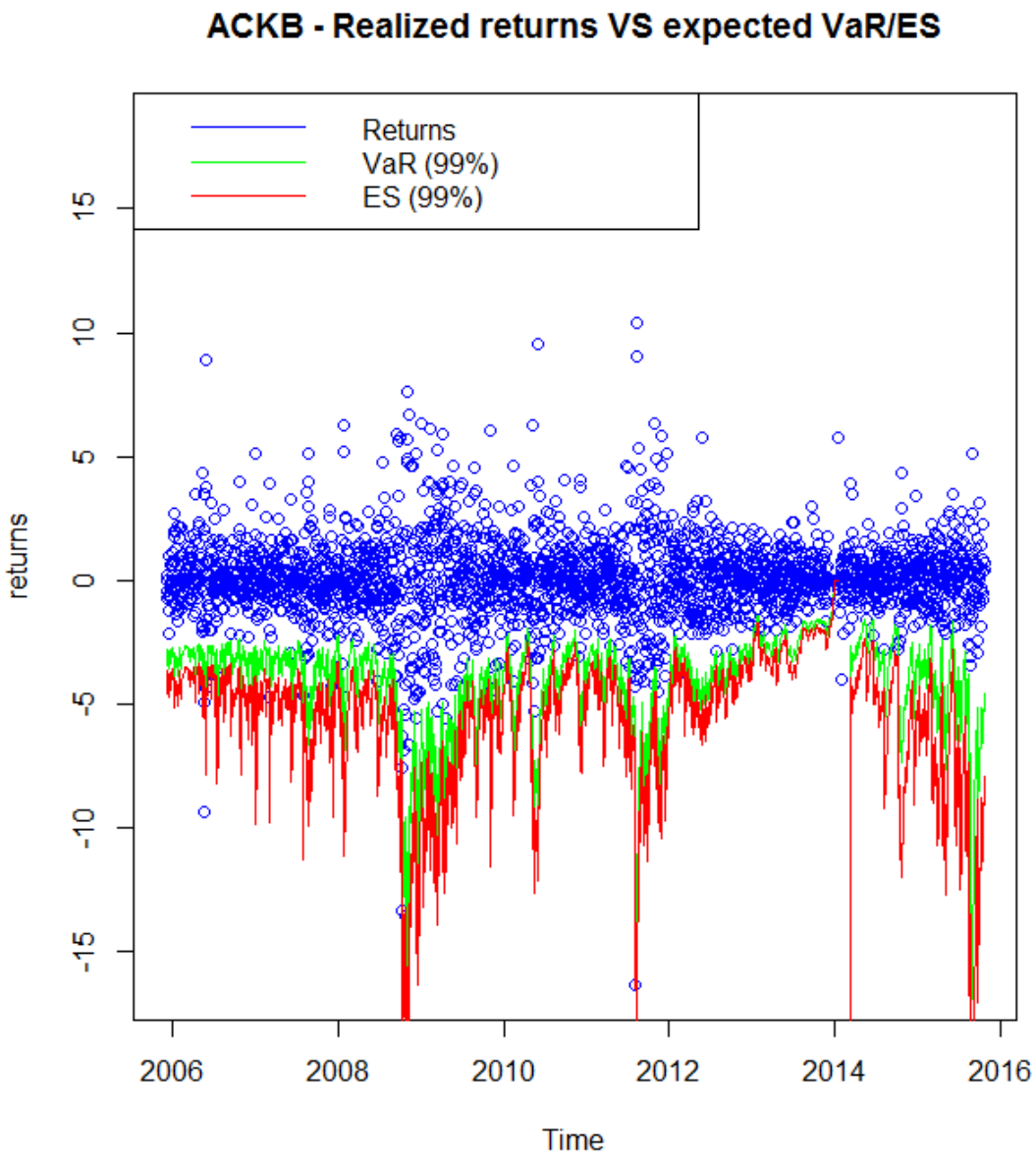

Figure 5.2: Egarch - expected VaR / ES (ACKB)

Chapter 6

Managing portfolio risk

In this chapter we investigate the topic of multivariate financial risk modeling. We first demonstrate that the normal assumption is unsuitable for multivariate risk forecasting and that the correlation coefficient is inappropriate as a dependency measure between two assets. As a better alternative, we illustrate how copulae can be combined with the techniques from the previous chapters as a means of measuring and managing the market risk of a portfolio. More concretely, a mixed EGARCH-Copula-Gumbel model is proposed as a reliable portfolio risk management tool.

6.1 Inadequacy of the correlation dependency measure

The pearson correlation coefficient depicts the strength of a linear relationship between two random variables and is defined as follows:

$$\rho(X_1, X_2) = \frac{Cov(X_1, X_2)}{\sqrt{Var(X_1)}\sqrt{Var(X_2)}} \tag{6.1}$$

with $Cov(X_1, X_2) = E[(X_1 - E(X_1))(X_2 - E(X_2))]$ the covariance between the random variables and $Var(X_1)$ and $Var(X_2)$ their variances.

Many potential problems can occur when employing the correlation as a measure of dependence. First, the dependency between two assets can only be captured adequately when their distributions are jointly elliptically distributed. Additionally, the linear correlation coefficient is not invariant with respect to non-linear random variables or if non-linear dependence between variables exists. As an example, consider $X_1 \sim \mathcal{N}(0, 1)$ and $X_2 = X_1^2$. There is obviously a direct relationship between these two variables, but their correlation value evaluates to 0. Indeed, $Cov(X_1, X_2) = E[X_1 \cdot (X_1^2 - 2)] = E(X_1^3) - E(X_1) = 0$ implies independence between X_1 and X_2 . Furthermore, The correlation coefficient also depends on the marginal distributions of the random variables and the possibility exists that not all values in the range $[-1, 1]$ are obtainable. As a result of these issues it becomes evident that we need alternative concepts for measuring dependence between risk factors.

6.2 A better alternative: Copulae

6.2.1 Theoretical overview

In the previous section we argued that the value of the correlation coefficient is dependent upon the marginal distributions. Hence, it is necessary to separate the marginal distributions from the dependency structure between the random variables; This kind of separation can be achieved by means of copula dependency modeling. The copula approach was introduced by Sklar (1959)[20] and detailed textbook exhibitions can be found in Schweizer and Sklar (1983)[21] and more recently in McNeil et al. (2005)[5]. Although the statistical concepts have been in circulation for more than half a century they have only recently been applied to model dependencies between assets in empirical finance.

Copulas are based upon elementwise transformations of the random vector $X = (X_1, .., X_d)$ such that the resulting variables follow a uniform distribution $U(0, 1)$. Given the assumption that all distribution functions $F_1, ..., F_n$ of the random vector X are continuous, this projection is given by the probability integral: $\mathbb{R}^d \to \mathbb{R}^d, (x_1, ..., x_n)^t \to (F_1(x_1), ..., F_d(x_d))^t$. The joint density function C of the transformed random variables $(F1(x1), ..., Fd(xd))^t$ is the copula of the vector $X = (X_1, ..., X_d)$:

$$
\begin{aligned}
F(x_1, ..., x_d) &= P[X_1 \leq x_1, ..., X_d \leq x_d] && (6.2)\\
&= P[F_1 \leq F_1(x_1), ..., F_d(X_d) \leq F_d(x_d)] && (6.3)\\
&= C(F_1(x_1), ..., F_d(x_d) && (6.4)
\end{aligned}
$$

Hence, a copula is the distribution function in $\mathbb{R}^d$ space of a d-element random vector with standard uniform marginal distributions U(0, 1). If the marginal distributions are continuous, then the copula is uniquely defined and it is possible to employ different distributions for the random variables as marginals and capture their dependencies with a copula. For example, the distributions introduced in the previous chapters classify as potential candidates for modeling the marginal risk factors of the joint portfolio distribution.

Another concept that is of great importance during the risk assessment of a portfolio is the tail dependence measure. This measure focuses only on the tails of the joint distribution and aims to determine the likelihood that 'extreme tail events' occur simultaneously for multiple marginals. The upper and lower tail dependencies for two random variables (X, Y) with marginal distributions F_X and F_Y are defined as

$$
\begin{aligned}
\lambda_u &= \lim_{q \to 1} P(Y > F_Y^{-1}(q) | X > F_X^{-1}(q)), && (6.5)\\
\lambda_l &= \lim_{q \to 0} P(Y \leq F_Y^{-1}(q) | X \leq F_X^{-1}(q)) && (6.6)
\end{aligned}
$$

Hence, tail dependence can be interpreted as the conditional likelihood of observing a great (small) value for Y, given a great (small) value for X. if $\lambda_u > 0$ then there is upper tail dependence between the two random variables, and if $\lambda_l > 0$ then there is lower tail dependence. Note that according to Bayes, we can rewrite the previous expressions as follows:

$$\lambda_l = \lim_{q \to 0} \frac{P(Y \leq F_Y^{-1}(q) | X \leq F_X^{-1}(q))}{P(X \leq F_X^{-1}(q))} = \lim_{q \to 0} \frac{C(q,q)}{q} \tag{6.7}$$

$$\lambda_u = 2 + \lim_{q \to 0} \frac{C(1-q, 1-q) - 1}{q}, \tag{6.8}$$

6.2.2 Classification of copulae

copulae can be classified into two broad categories. The first category are the distribution based copula and they aim to capture the dependency structure between the random variables with their distribution parameters. Examples of closed form distribution based copula are the Gauss copula, which implies zero tail dependency and the t copula which has a coefficient of tail dependence that is defined as follows:

$$\lambda_u = \lambda_l = 2t_{v+1}(-\sqrt{v+1}\sqrt{\frac{1-\rho}{1+\rho}}) \tag{6.9}$$

The advantages of distribution-based copula lie in their simplicity and the fact that simulations can be carried out easily. The main disadvantage of such models is that large parameter constellations must be estimated during the calibration process and that closed-form solutions can not be derived. Furthermore, in the case of elliptical distributions, the assumed symmetry fails to capture the empirical skewness of asset returns. Hence, such distributions are not adequate for risk modeling purposes.

The second category are the archimedian copula and they can be defined as follows:

$$C(u_1, u_2) = \psi^{-1}(\psi(u_1) + \psi(u_2)) \tag{6.10}$$

where ψ is the so called copula-generating function. A well known example of an Archimedian copula is the Clayton copula and its copula generating function can be written as follows:

$$\psi(t) = \frac{(t^{-\delta} - 1)}{\delta}, \quad \delta \in (0, \infty) \tag{6.11}$$

For $\delta \to \infty$ a perfect dependency results while for $\delta \to 0$ independence is obtained. Furthermore, the Clayton copula possesses lower tail dependence with a corresponding value of $\lambda_l = 2^{-1/\delta}$. The Gumbel copula is another important Archimedian copula and its copula-generating function is defined as $\psi(t) = -ln(t)^\theta$ with $\theta \geq 1$. The Gumbel copula possesses upper tail dependence. Perfect dependence exists for $\theta \to \infty$ and independence for $\delta \to 1$. The coefficient of tail dependence can be determined according to $\lambda_u = 2 - 2^{-1/\theta}$.

In contrast to the distribution based copulae, Archimedian copulae contain a closed form distribution. Furthermore, a wide range of dependency structures can be modelled with them. On the other hand, their main drawback is their complex structure for higher multivariate dimensions. However, as we will illustrate in the next subsection, this problem can be circumvented by using a nested two-step modelling design.

6.3 Risk modeling application

6.3.1 The mixed EGARCH-Clayton-Gumbel copula model

In this section, we investigate a class of models that can simultaneously address the univariate and multivariate stylistic features of asset returns in a global portfolio context. Such models allow a portfolio manager to measure and assess portfolio wide risk in an effective and reliable manner. In order to achieve this goal, we put the pieces from the previous chapters together by combining the univariate modeling power of (E)GARCH with the multivariate copula dependency modeling capabilities. The multivariate return series under consideration consist of the 9 SPDR ETF funds and 14 BEL20 stocks, as they are illustrated in figure 6.1 and 6.3. Boxplots of the corresponding asset returns are displayed in figure 6.2 and figure 6.4.

6.3.2 Calibration and risk forecasting

In the example that follows we illustrate the calibration process for a mixed EGARCH-Clayton-Gumbel model and subsequently utilize the model as a risk forecasting tool at the portfolio level. To achieve this goal, we employ a two step estimation approach, as proposed by Joe and Xu (1996)[22] and shih and Louis (1995)[23]. During the first step of the process, we use an ARMA-EGARCH specification to model the individual return series marginals (equations 5.8-5.12). Note that we use the same model specification as before and employ a standardized skewed t distribution to model the error component $\mathcal{D}_{k,v}(0,1)$. Next, the standardized residuals for each of the resulting EGARCH models are computed as $\hat{z_{k,t}} = \frac{(x_{k,t}-\hat{\mu_{k,t}})}{\hat{\sigma_{k,t}}}$, where the k parameter represents the kth financial asset in the portfolio. Figure 6.5 and figure 6.6 illustrate some of the quantile-quantile plots for these standardized residuals versus the theoretical counterparts of the fitted conditional error distributions. As we discussed previously, the EGARCH models provide a good fit for the individual marginals. Next, we use the conditional distributions from the fitted EGARCH models to generate pseudo-uniform variables from the standardized residuals. In the second step of the calibration process, the resulting pseudo-uniform variables are utilized to maximize the copula-likelihood. Here, we choose to calibrate a mixed Clayton-Gumbel copula due to its ability to effectively model both the upper and the lower tail dependency between the individual return series.

Now that the calibration process is finished, we can use the resulting dependency structure to derive risk measures for any given confidence level, by simulation. This

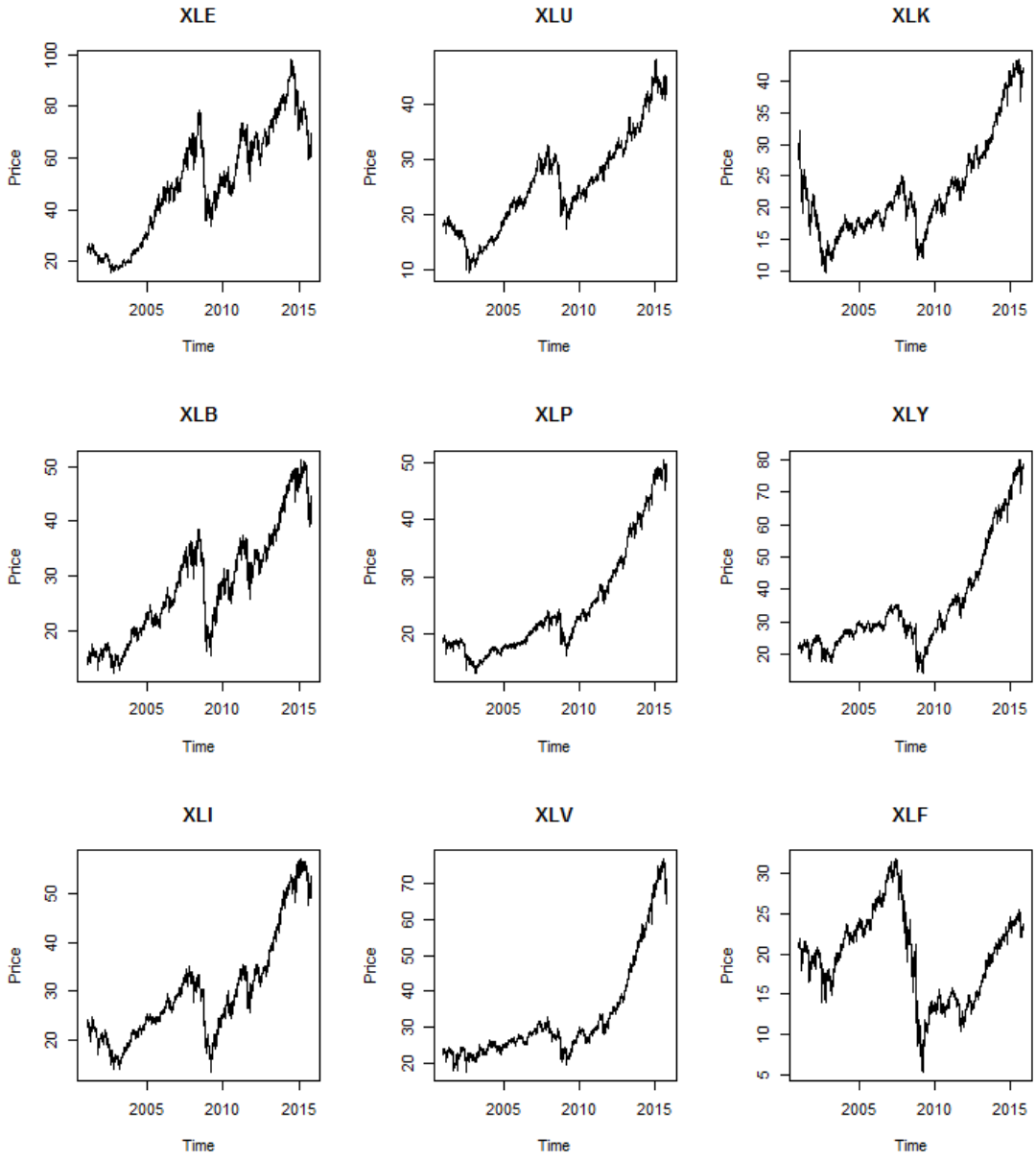

Figure 6.1: SPDR ETF Timeseries

process entails generating M data sets of random variates for the pseudo-uniformly distributed variables and subsequently employing the conditional distribution functions from the EGARCH models to obtain their respective quantile values. These quantile values are then used in conjunction with the weight vector and the one day ahead forecasted μ and σ values to calculate M portfolio return scenarios from which the risk measures

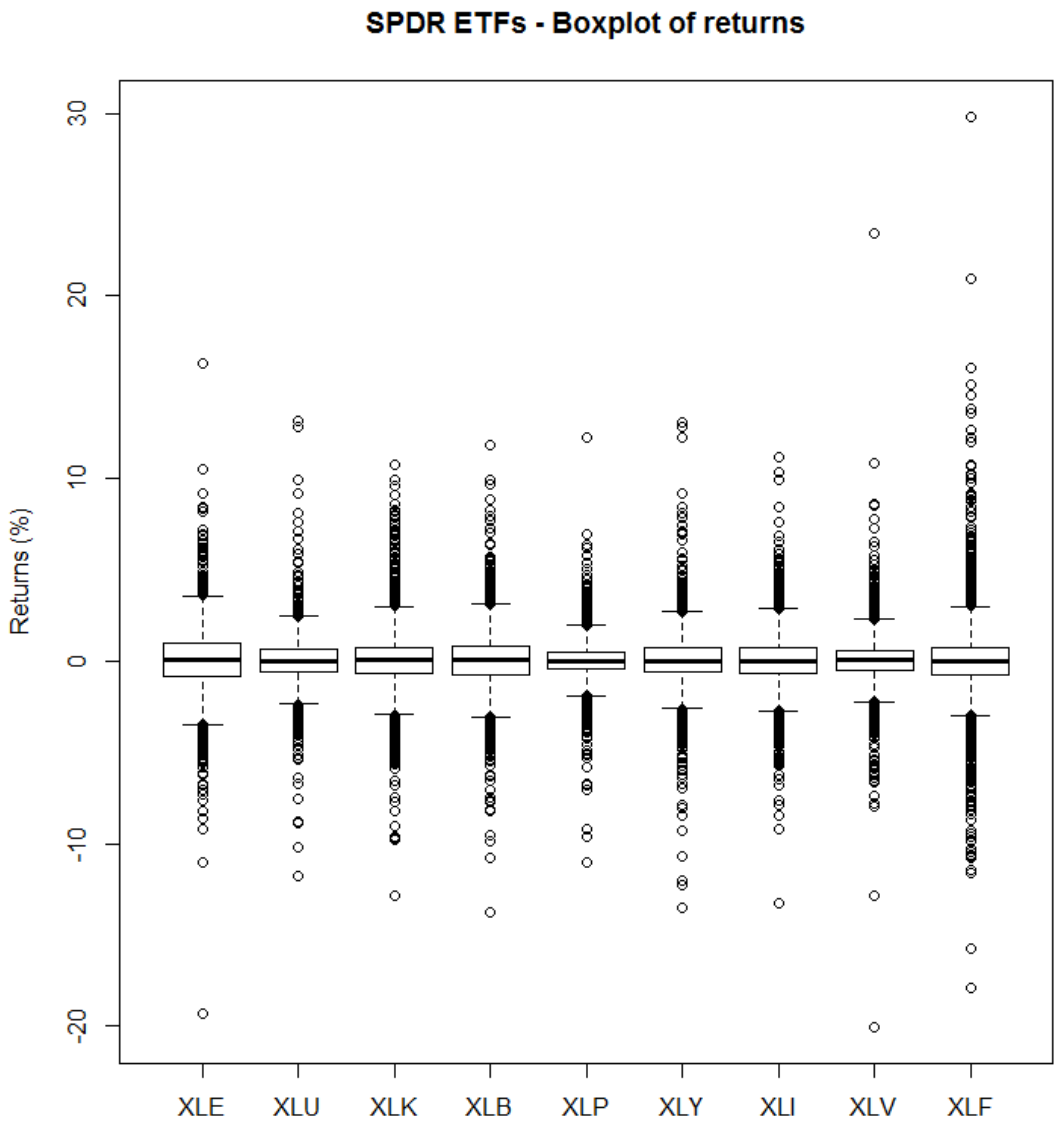

Figure 6.2: SPDR ETFs - Boxplot of return data

can be derived empirically. The calibration and risk forecasting process is illustrated in figure 6.7.

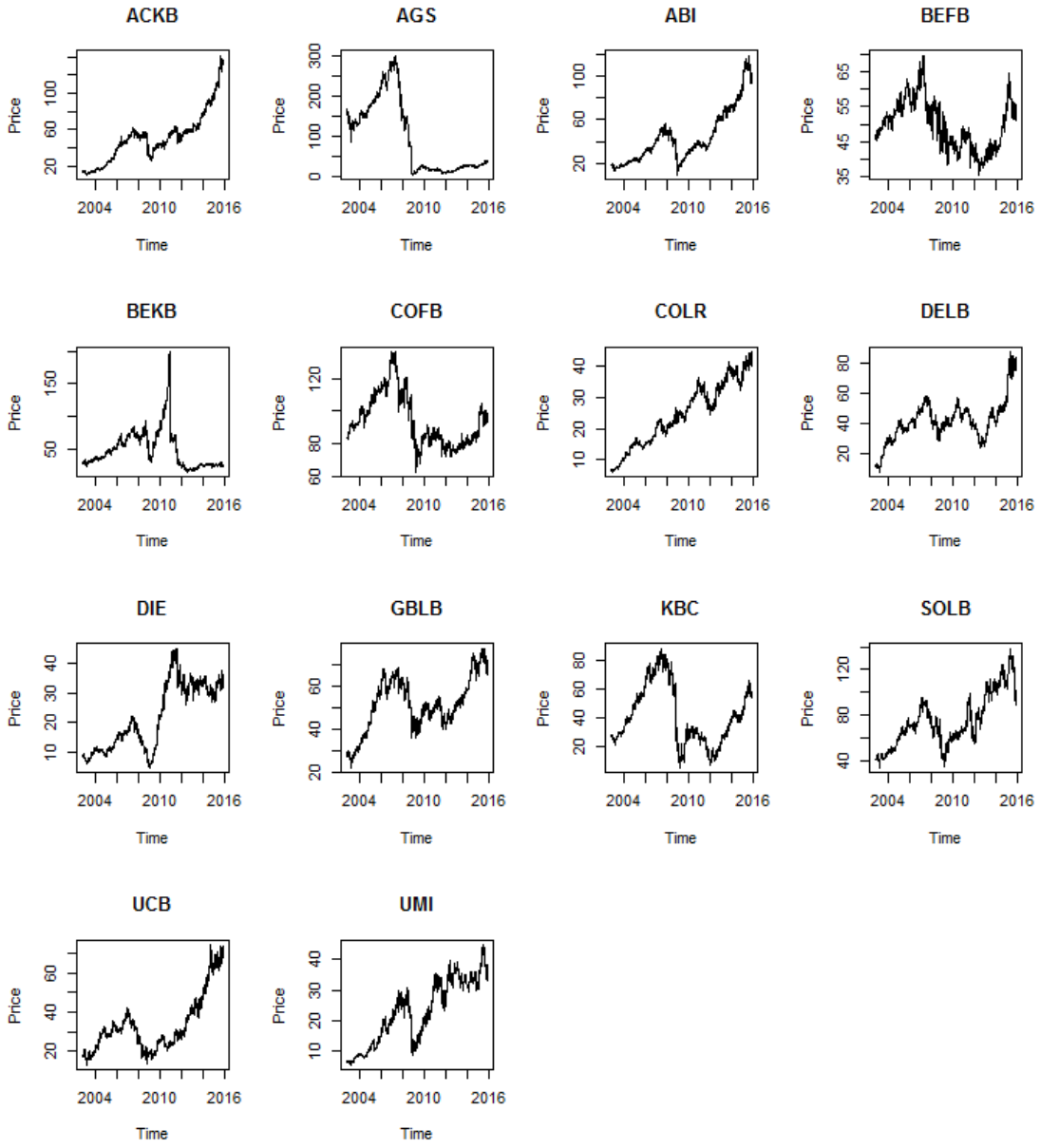

Figure 6.3: BEL20 Timeseries

6.3.3 Performance evaluation

Next, We evaluate the performance of the EGARCH-Clayton-Gumbel model by conducting a VaR and ES forecasting backtest on the SPDR ETF portfolio. We use a moving window of 375 datapoints and assume an equal weight asset allocation between the 9 ETF funds. The EGARCH-Clayton-Gumbel model is only recalibrated every 10

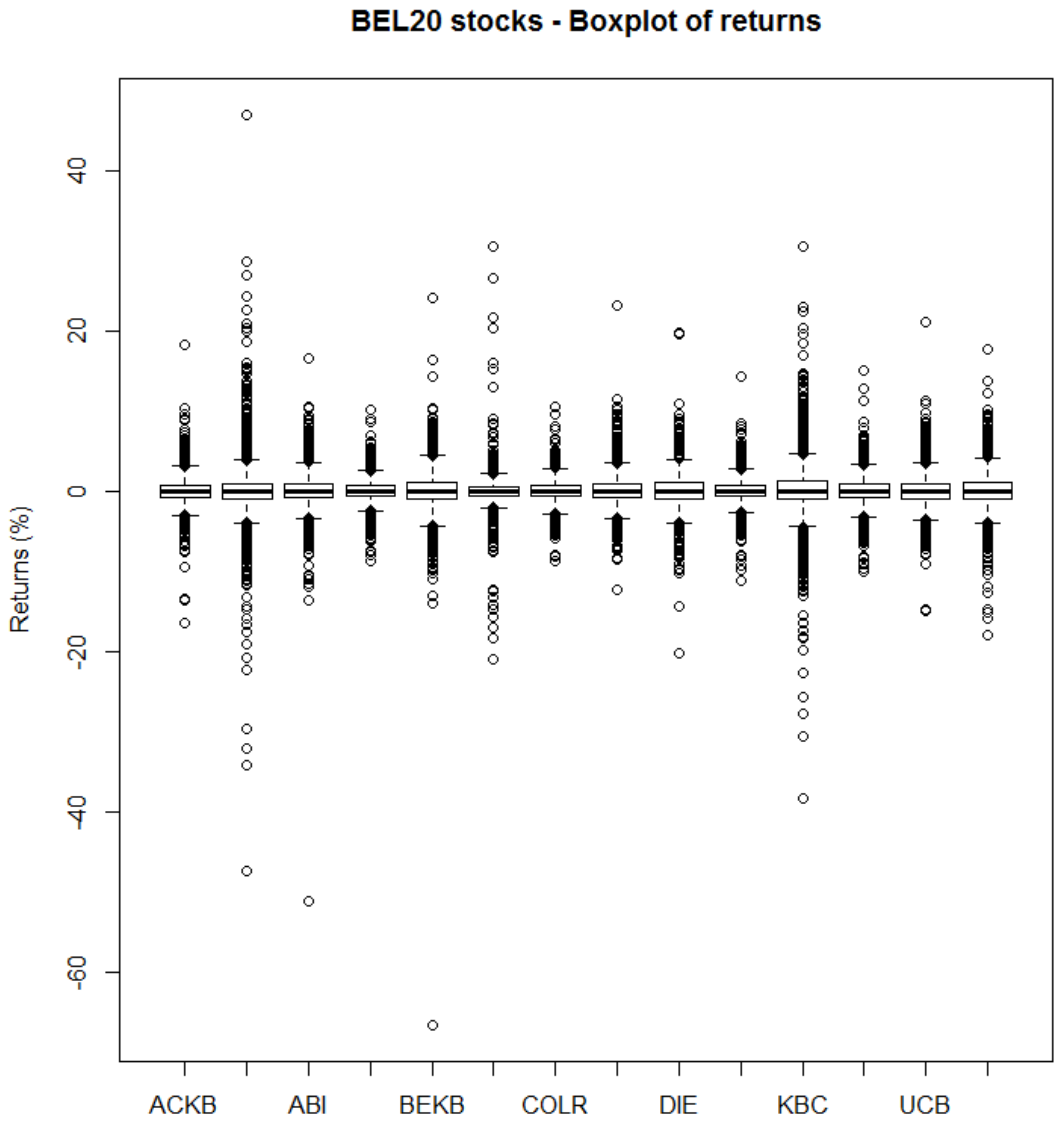

Figure 6.4: BEL20 Stocks - Boxplot of return data

days for performance reasons but new volatility and risk forecasts are made on a daily basis for the marginals. The left top graphs in figure 6.8 illustrates the results of the equal asset allocation backtest. The top right graphs shows the expected VaR and ES and a VaRtest demonstrates that the null hypothesis of correct amount of exceedances can not be rejected; There were 37 violations of the porftolio VaR while 34 exceedances

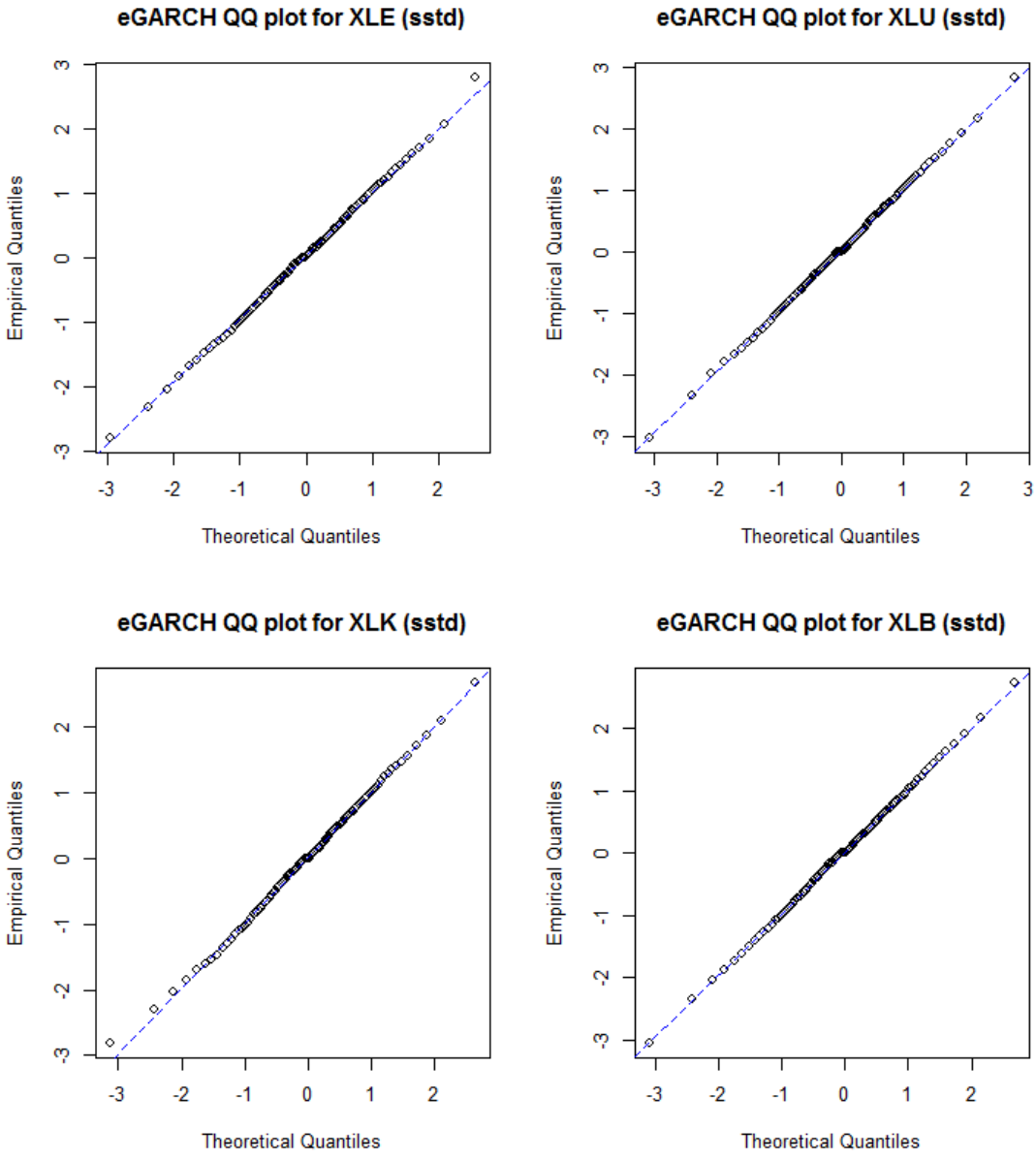

Figure 6.5: EGARCH (SPY) - Standardized residuals versus conditional distribution

were expected. The bottom left graph illustrates the performance results when weights are rescaled in such a way that an expected next day VaR level of 2% is targeted. In practice, this will effectively downscale the positions when excessive volatility is detected and have the reverse effect during more tranquil periods. The results also demonstrate that this VaR targetting approach has the potential to significantly improve portfolio

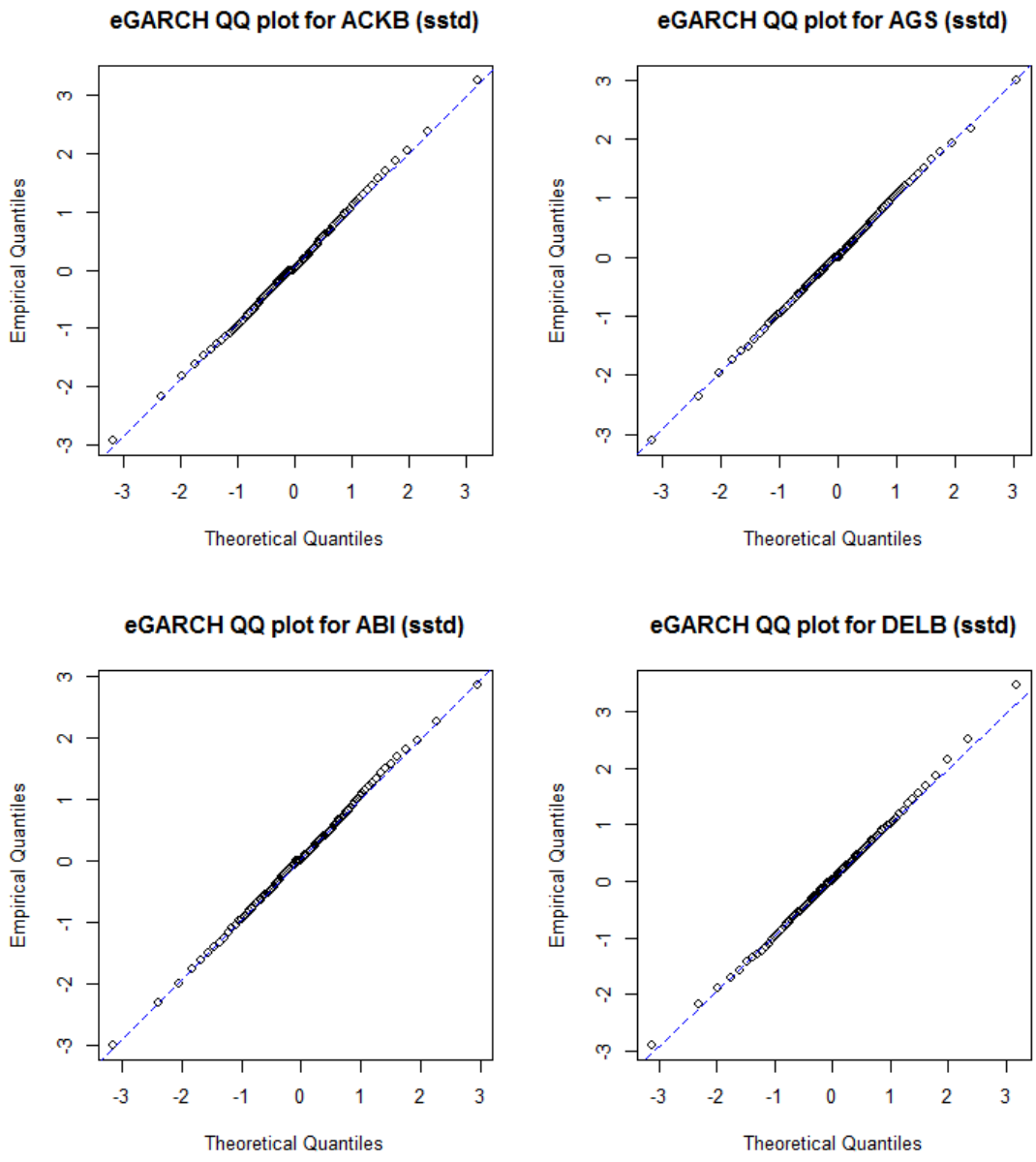

Figure 6.6: EGARCH (BEL20) - Standardized residuals versus conditional distribution

performance: The equal weights strategy has a sharpe ratio of 0.51 while the same strategy with a VaR targetting approach shows a sharpe ratio of 0.61.

Finally, we repeat the process on the BEL20 stock portfolio and illustrate the results in figure 6.9. We encountered 34 violations of the portfolio VaR while 30 were expected. We note that the returns of this portfolio are very volatile but we manage to succesfully

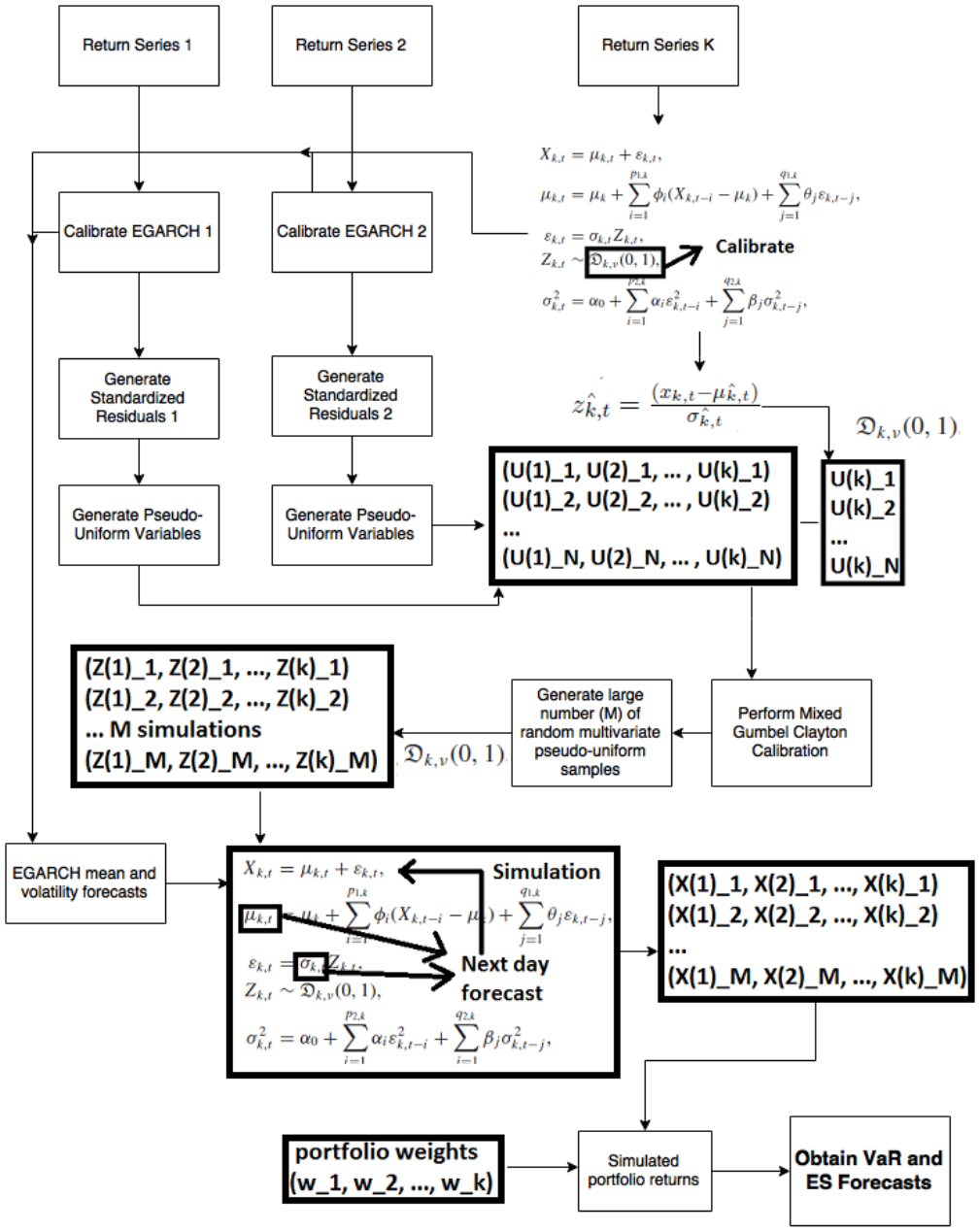

Figure 6.7: EGARCH-Clayton-Gumbel - Calibration Process and Risk Forecasting

mitigate downside risk by employing the EGARCH-Clayton-Gumbel VaR targeting tool. As an added bonus, trading performance is significanatly improved with the sharpe ratio increasing from around 0.6 to 1.01.

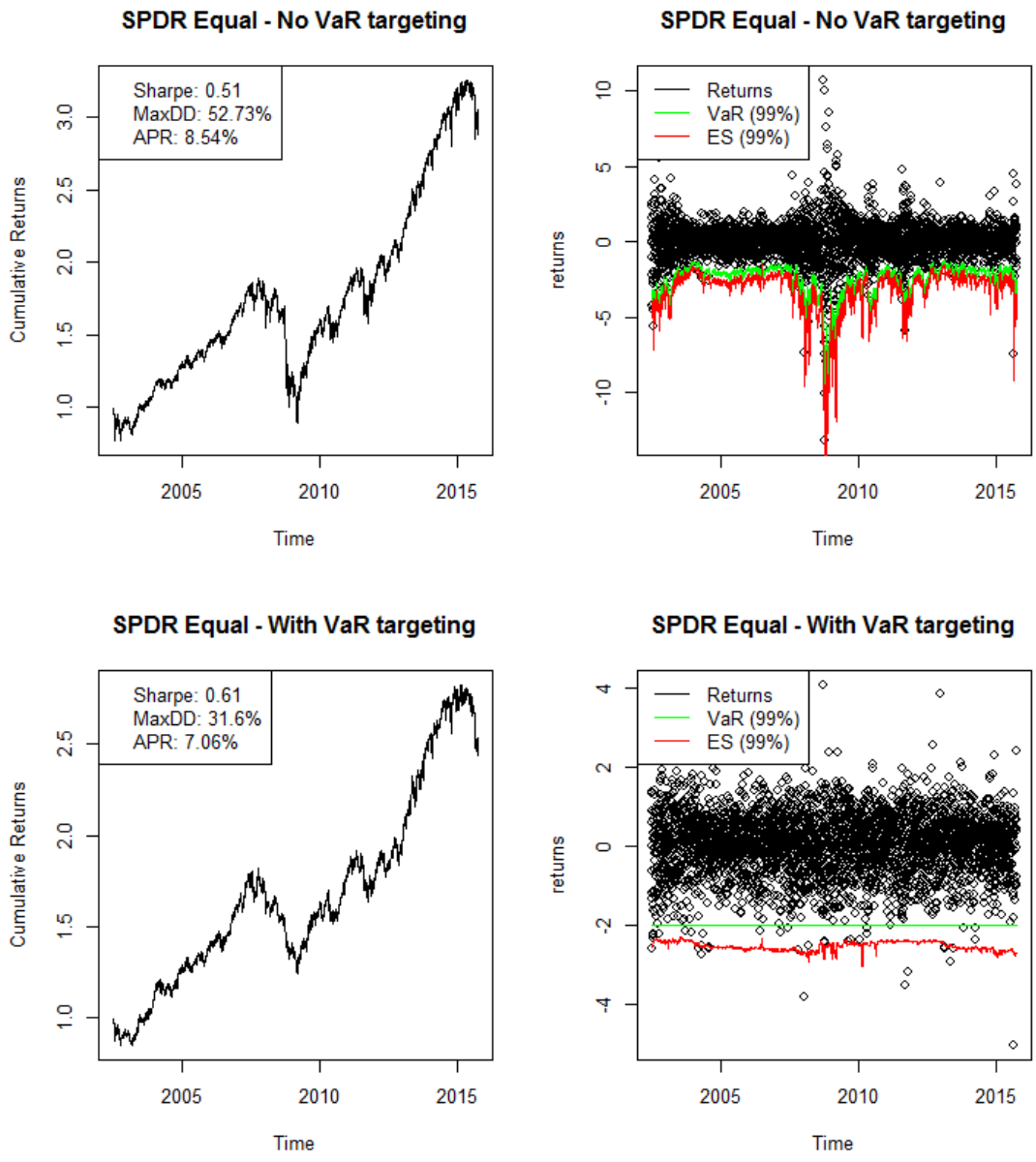

Figure 6.8: SPDR ETF Portfolio - Equal Weigths Allocation

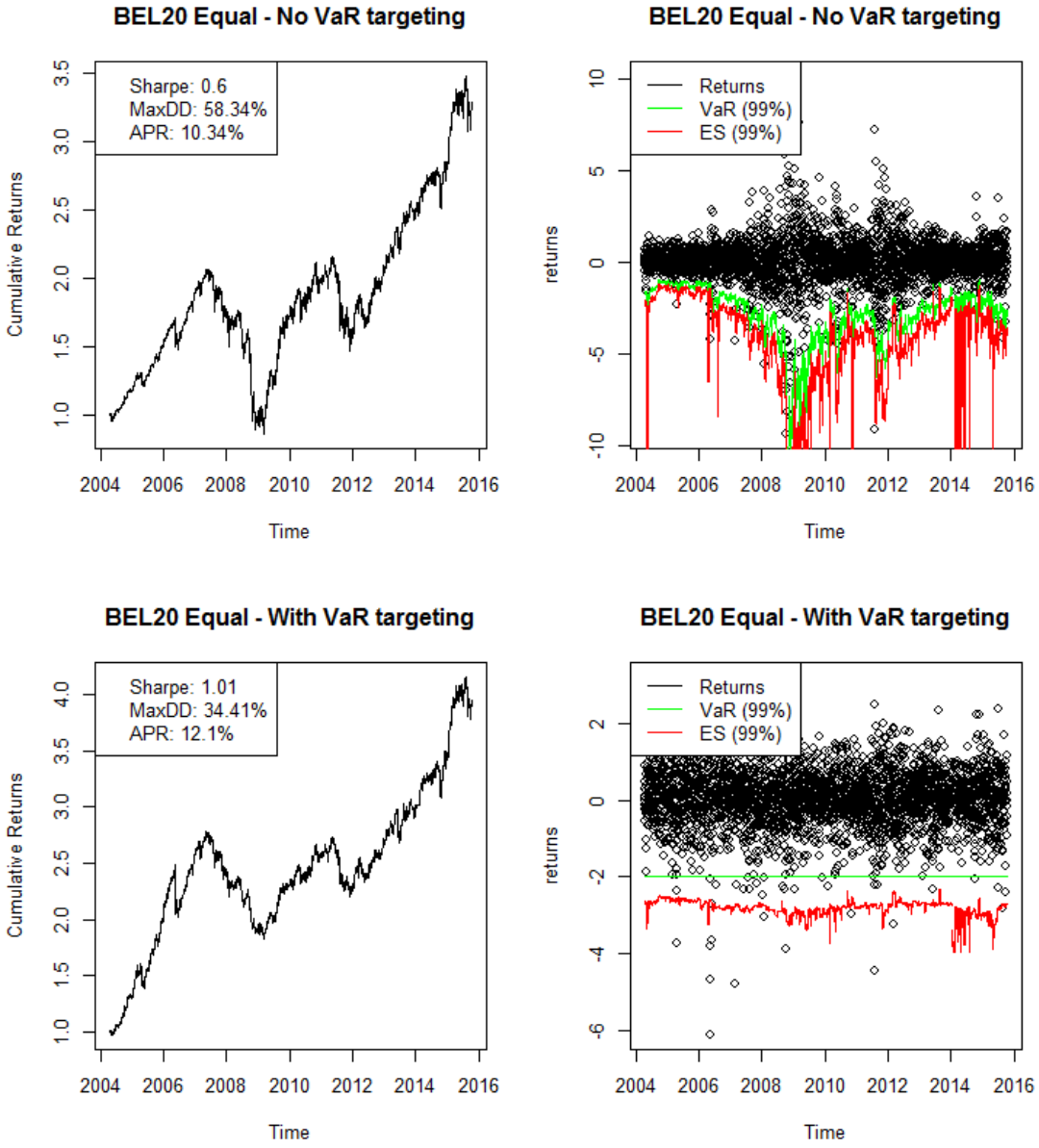

Figure 6.9: BEL20 Stock Portfolio - Equal Weights Allocation

Chapter 7

Practical Application - Trading strategy risk management

In this chapter we use the EGARCH-Clayton-Gumbel tool to manage trading strategy risk exposure. More concretely, we apply VaR targeting to periodically rebalance the portfolio target weights: This allows a portfolio manager to obtain a constant expected risk exposure over time.

7.1 Trading rules

The trading rules of the strategy under consideration are defined as follows: We determine the direction (long/short) of the underlying assets by looking at the value of a short term (50 days) exponential moving average (EMA) relative to the value of a longer term (200 days) moving average. If the short term EMA value is larger than the longer term EMA value then we are long the asset, otherwise we short the asset. The initial relative weights of the securities are volatility weighted such that $w_i = \frac{1}{\sigma_i}$ for long positions and $w_i = -\frac{1}{\sigma_i}$ for short positions, where σ_i represents the daily volatility of asset i over the previous 200 days. The weights are subequently normalized such that $w_i = \frac{w_i}{\sum_{j=1}^{n} |w_j|}$. We perform daily rebalancing of weights, given the updated volatility structure.

7.2 Performance evaluation

The trading results are illustrated in figures 7.1 and 7.2 for the SPDR ETF index and BEL20 stock portfolios respectively. The top graphs show the trading results (left) and next day risk forecasts (right) when no VaR targeting is applied. In contrast, the bottom graph shows results when weights are rescaled in such a way that a 2% expected next-day VaR value is targeted. As we concluded before, the VaR targeting tool succesfully mitigated downside risk and has the potential to significantly improve overall trading strategy performance.

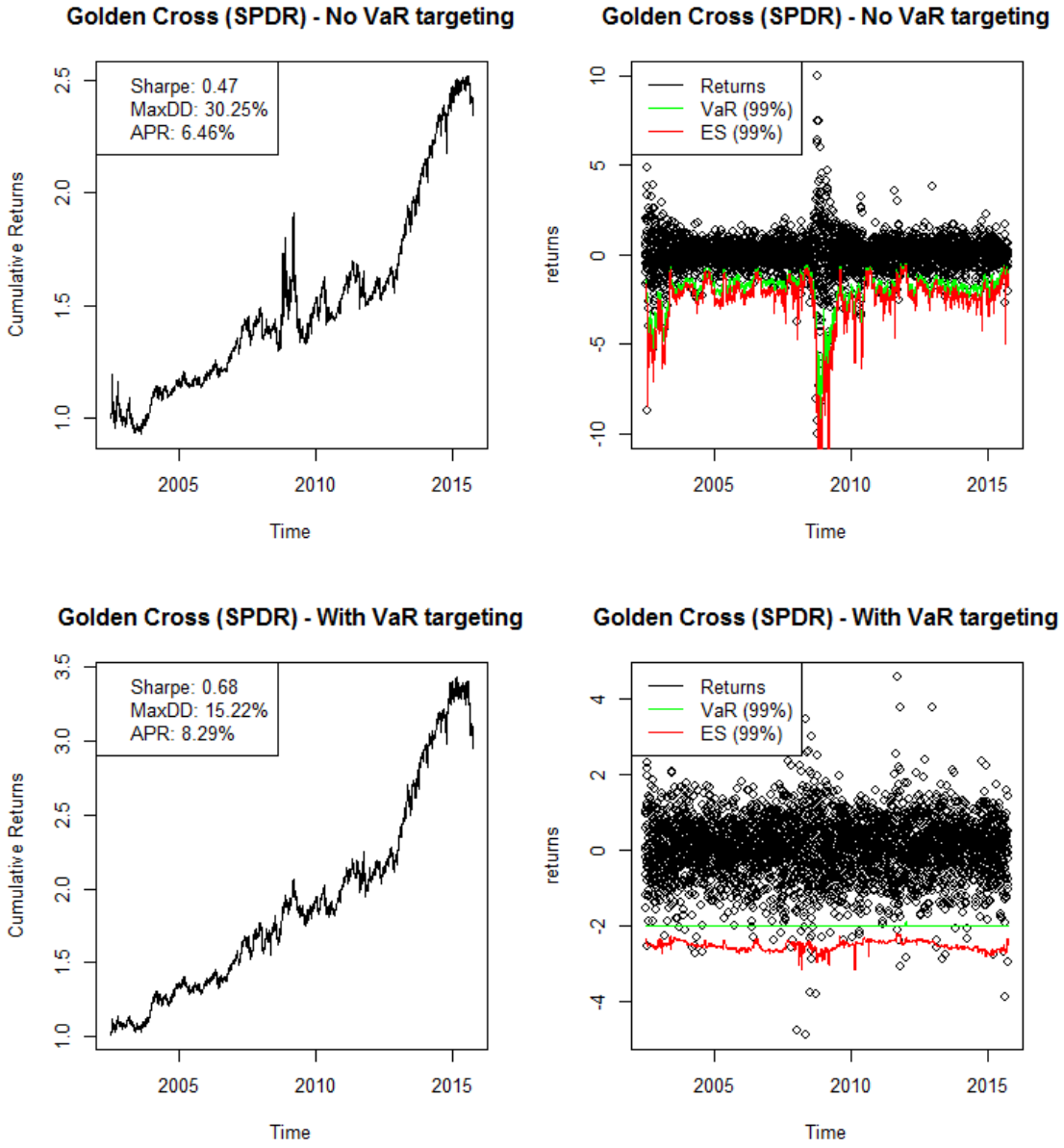

Figure 7.1: Trading Strategy - SPDR ETF Results

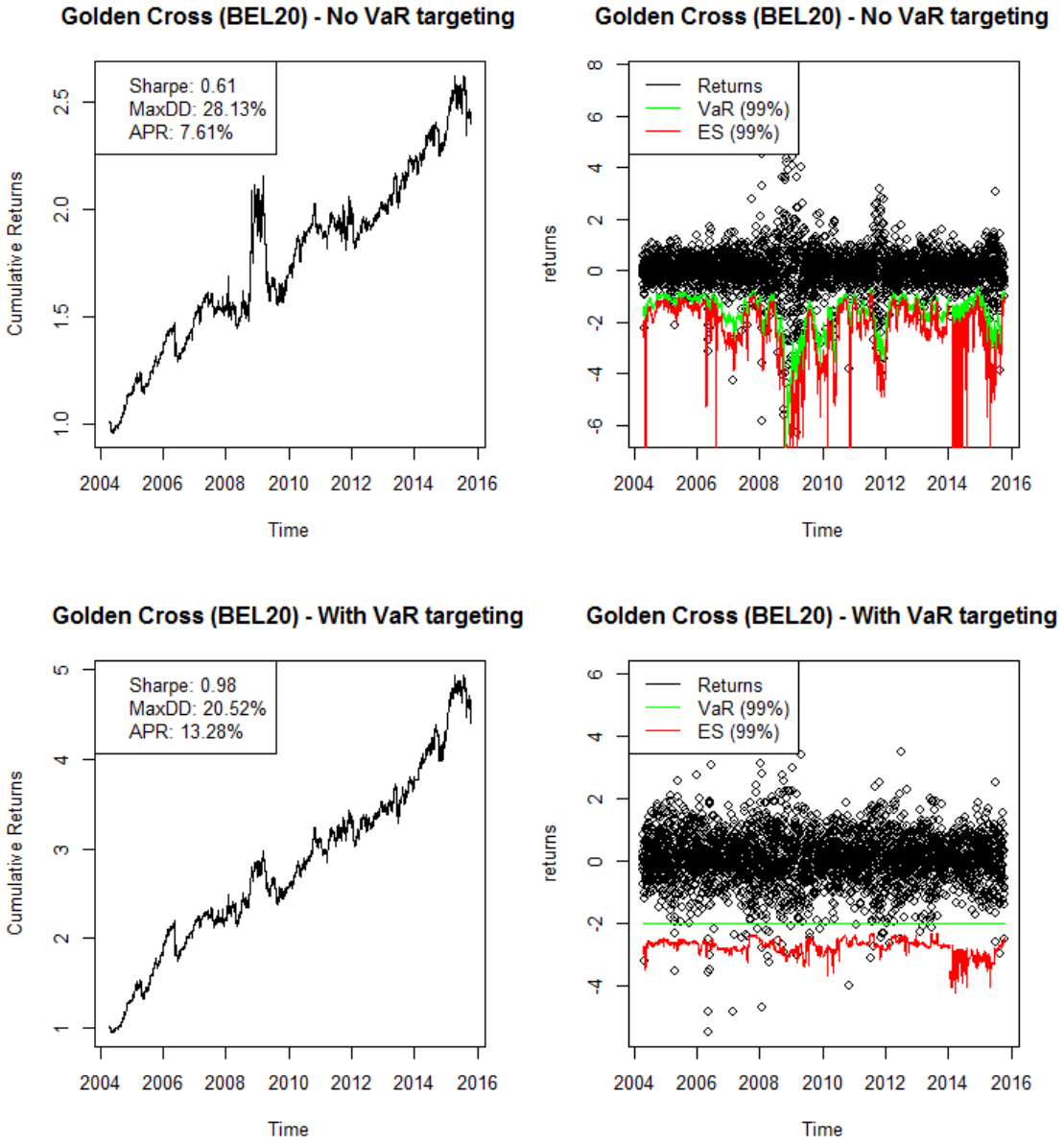

Figure 7.2: Trading Strategy - BEL20 Stock Results

Bibliography

[1] Markowitz H. (1952). Portfolio selection *Journal of Finance* **7**, no. 7(1), 77–99

[2] Pfaff B. (2013). Financial Risk Modelling and Portfolio Optimization with R. Wiley, New York.

[3] Fabozzii F.J., Kolm P.N, Pachamanova D.A and Focardi S.M (2007). Robust Portfolio Optimization and Management. Wiley, New York.

[4] Campbell J., Lo A.and MacKinlay A. (1997). The Econometrics of Financial Markets. *Princeton University Press, Princeton, NJ.*

[5] McNeil A. and Embrechts P. (2005). Quantitative Risk Management: Concepts, Techniques and Tools. *Princeton University Press, Princeton, NJ.*

[6] RiskMetrics Group (1994). Riskmetrics technical document. Technical report. *J.P. Morgan, New York.*

[7] Artzner P., Delbaen F., Eber J. and Heath D. (1997). Thinking coherently. *Risk*, no. 10(11), 68–71

[8] Artzner P. (1999). Coherent measures of risk *Mathematical Finance*, no. 9, 203-228

[9] Barndorff-Nielsen O. (1977). Exponential decreasing distributions for the logarithm of particle size. *Proceedings of the Royal Society London*, no. A 353, 401–419

[10] Eberlein E. and Keller U. (1995). Hyperbolic distributions in finance. *Bernoulli*, no.1, 281–299

[11] Christoffersen P. (1998). Evaluation Interval Forecasts *International Economic Review*, no 39, 841–862

[12] Christoffersen P., Hahn J., and Inoue A. (2001). Testing and Comparing Value-at-Risk Measures *Journal of Empirical Finance*, no. 8, 325–342

[13] McNeil A.J, Frey R. and Embrechts P. (2000). Estimation of tail-related risk measures for heteroscedastic financial time series: an extreme value approach. *Journal of Empirical Finance*, no. 7, 371–300

[14] Coles S. (2001). An Introduction to Statistical Modeling of Extreme Values *Springer-Verlag, London.*

[15] Embrechts P., Kluppelberg C and Miksoch T. (1997). Modelling Extremal Events for Insurance and Finance vol. 33 of Stochastic Modelling and Applied Probability *Springer-Verlag, Berlin.*

[16] Engle R. (1982). Autoregressive conditional heteroscedasticity with estimates of the variance of United Kingdom inflation. *Econometrica*, no. 50(4), 987-1007

[17] Engle R. and Bollerslev T. (1986). Modelling the persistence of conditional variances *Econometric reviews*, no. 5, 1-50

[18] Bollerslev T., Chou R. and Kraker K. (1992). ARCH modeling in finance. *Journal of econometrics*, no. 52, 5-59

[19] Bera A. and Higgins H. (1993). ARCH models: Properties, estimation and testing *Journal of Economic Surveys*, no. 7(4) 52, 305–362

[20] Sklar A. (1959). Fonctions de répartitions a n dimensions et leurs marges *Publications de l'Institut d l'Université de Paris*, no. 8, 229-231

[21] Schweizer B. and Sklar A. (1983). Probabilistic Metric Spaces. *North-Holland/Elsevier, New York.*

[22] Joe H. and Xu J. (1996). The estimation method of inference functions for margins for multivariate models. Technical report 166. *University of British Columbia, Department of Statistics*

[23] Shih J. and Louis T. (1995). Inferences on the association parameter in copula models for bivariate survival data. *Biometrics* , no. 51, 1384-1399

[24] Black F and Litterman R. (1990). Asset allocation: combining investor views with market equilibrium. Technical report, *Goldman Sachs Fixed Income Research*

[25] Meucci A. (2006). Beyond Black-Litterman in practice: A five-step recipe to input views on non-normal markets. *Risk* **7**, no. 19(9), 114–119

FACULTY OF BUSINESS AND ECONOMICS
Naamsestraat 69 bus 3500
3000 LEUVEN, BELGIË
tel. + 32 16 32 66 12
fax + 32 16 32 67 91
info@econ.kuleuven.be
www.econ.kuleuven.be